Strasbourg, 23 septembre 2005

Compaction, dilatance et modes de rupture dans les roches de la croûte

Patrick Baud

Habilitation à diriger des recherches

Laboratoire de Physique des Roches
Institut de Physique du Globe de Strasbourg, UMR CNRS-ULP 7516
Ecole et Observatoire des Sciences de la Terre
Université Louis Pasteur (Strasbourg I)

Ecole et Observatoire des Sciences de la Terre

UNIVERSITÉ LOUIS PASTEUR STRASBOURG

CENTRE NATIONAL DE LA RECHERCHE SCIENTIFIQUE

Thèmes de recherche

- transition fragile-ductile
- effet de l'eau
- anisotropie
- couplage déformation circulation de fluides
- bandes de compaction

Compaction localization in porous sandstone

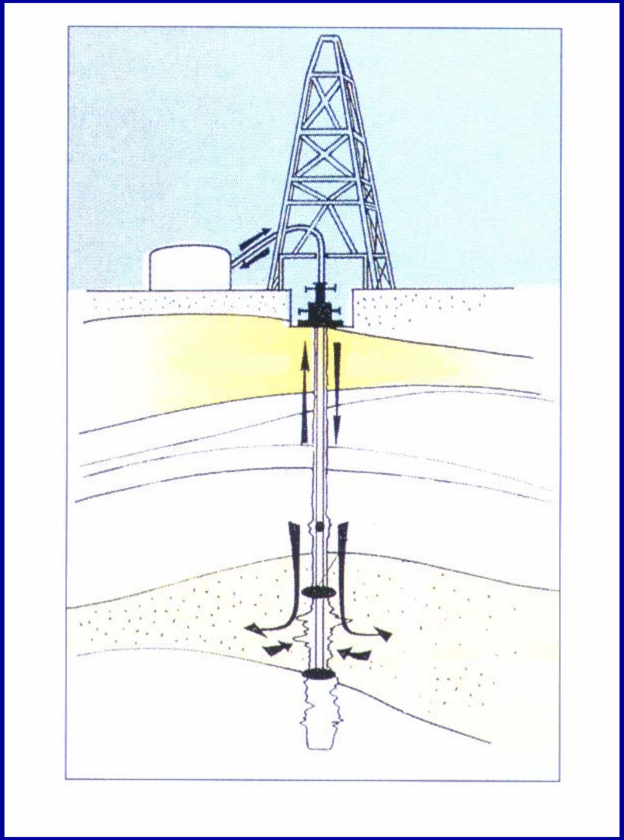

Consequences of oil production :

• failure

• subsidence

• permeability decrease

homogeneous/localized deformation (*compaction bands*)

→ Influence on fluid flow in reservoirs ?

Outline:

I. Field observations

II. Compaction in porous sandstones: result from previous studies

III. Laboratory observations of compaction localization

IV. Influence on fluid flow

V. Models

VI. Conclusions and future work

I. Field observations

Compaction bands
(Navajo sandstone, Utah)

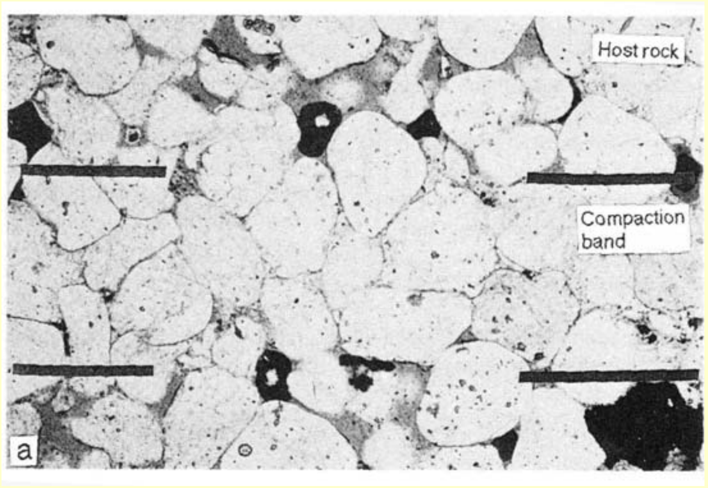

•purely compactive deformation

•bands orthogonal to major principal stress

Mollema and Antonellini (1996)

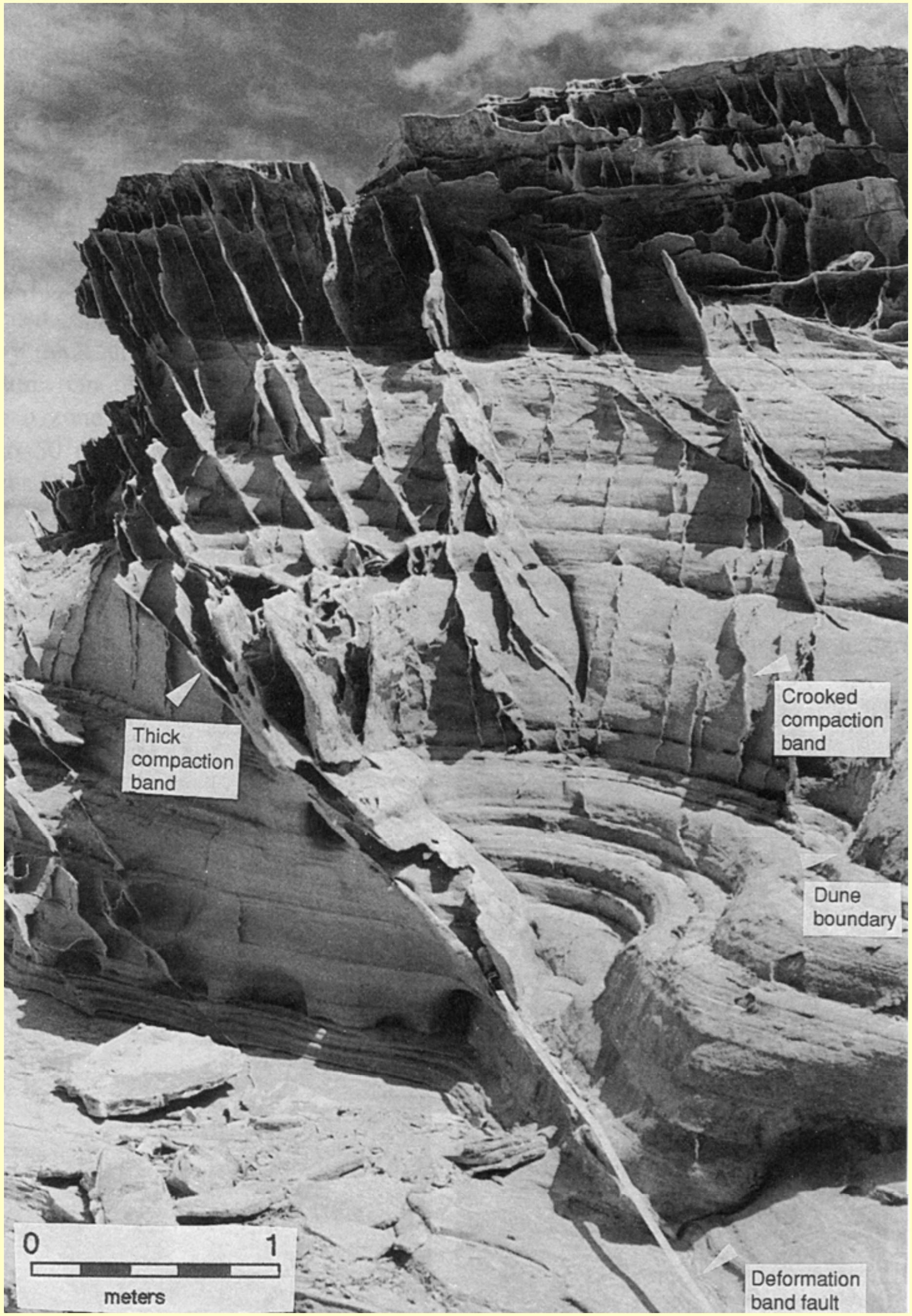

II. Compaction in porous sandstones: results from previous studies

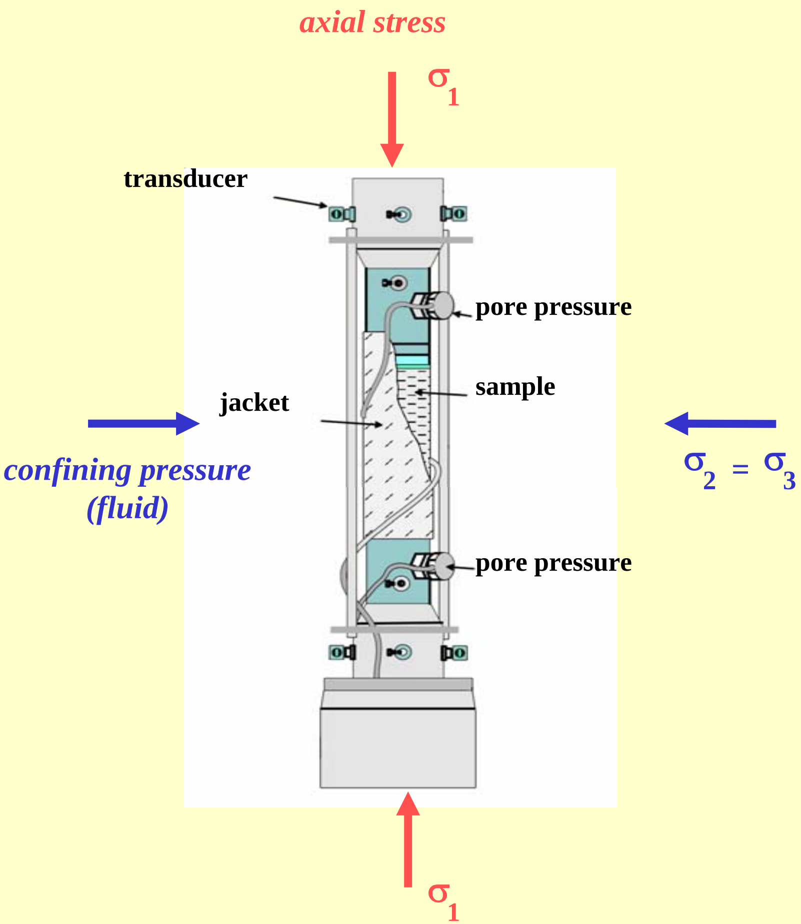

conventional triaxial experiments

- room temperature
- strain rate: 10^{-5}/s
- drained experiments: P_p = 10 MPa
- sample size: 40 mm x 20 mm

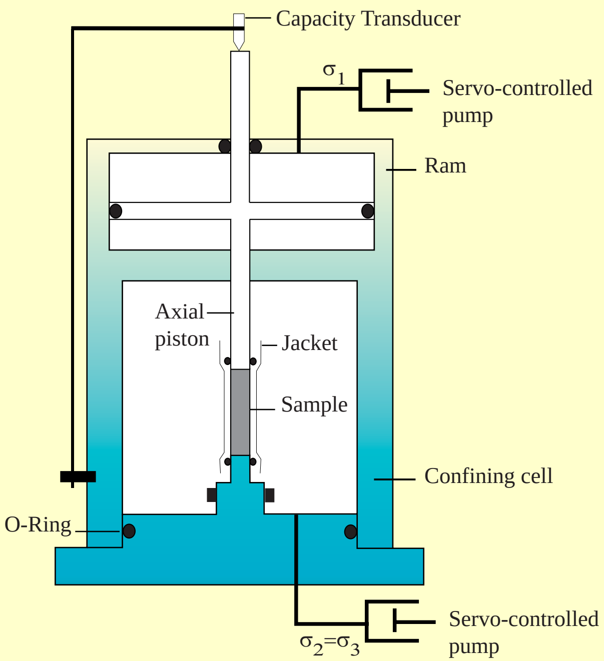

Two end-member failure modes

brittle faulting

- ***dilatancy***
- ***strain softening***
- ***shear localization***

ductile flow

- ***compaction***
- ***strain hardening***
- ***delocalized cataclastic flow***

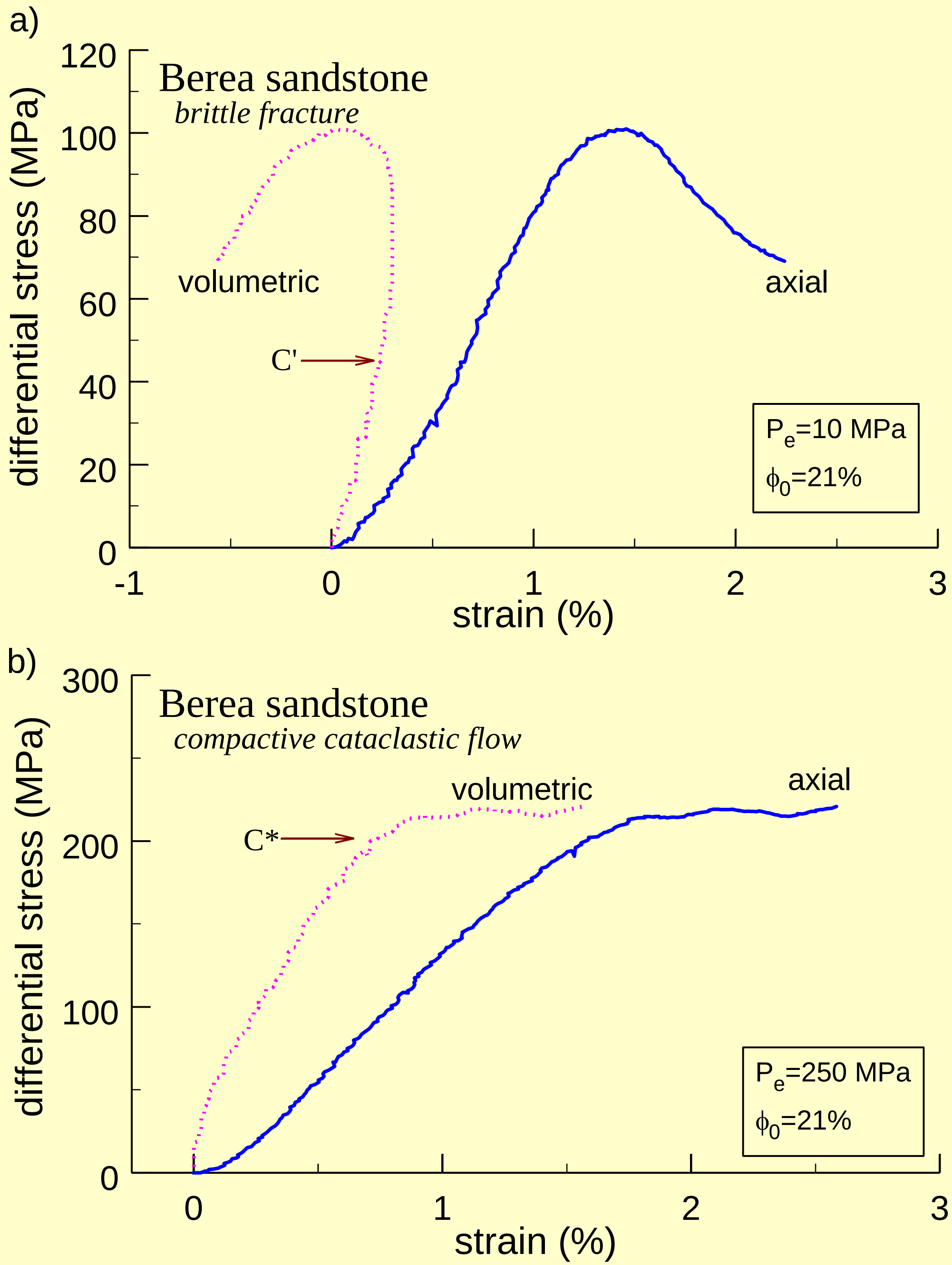

Zhu and Wong (1997)

Quantitative Stereology and Spatial Distribution of Damage

- *specific crack surface area S_v*
- *stress-induced anisotropy ω*
- *chord length distribution*

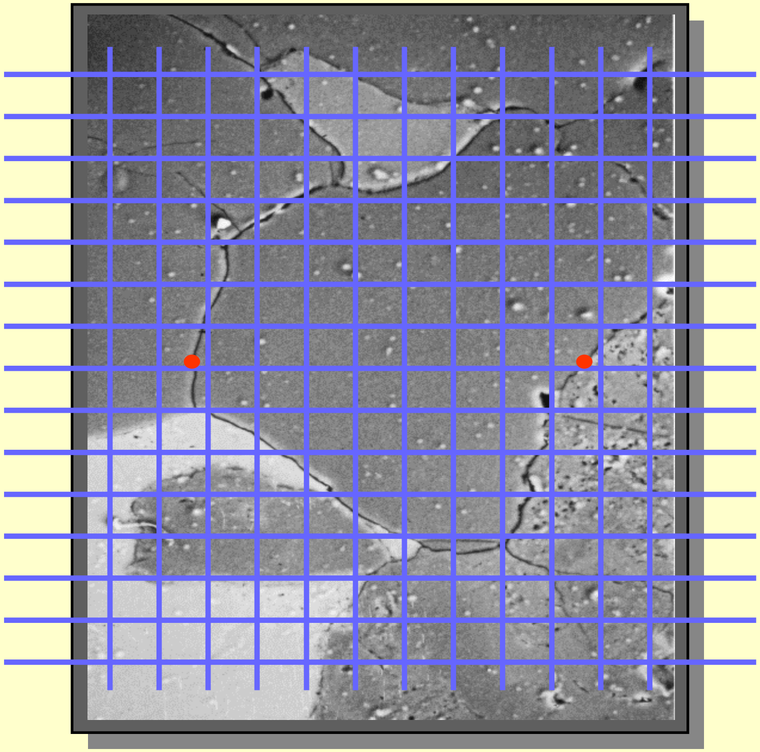

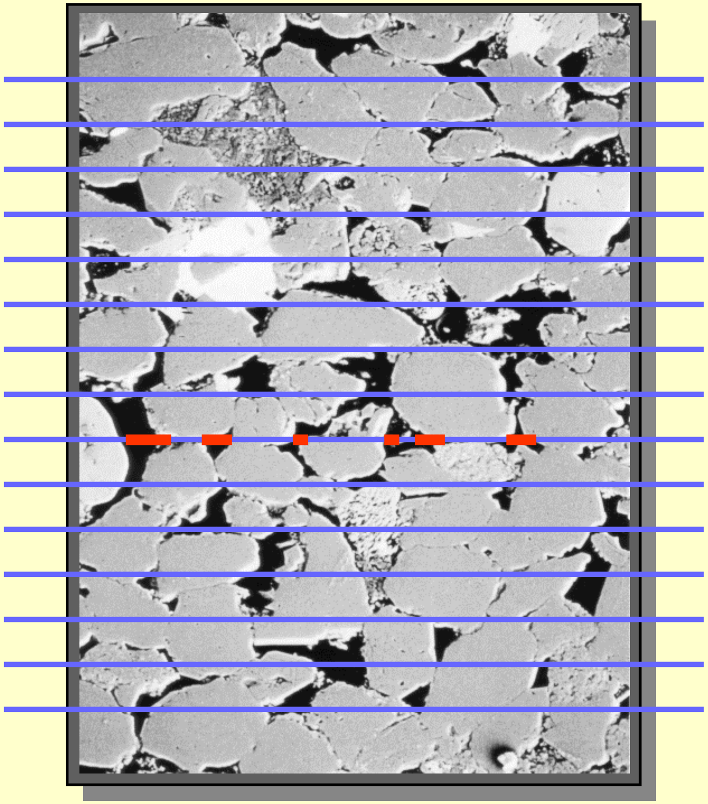

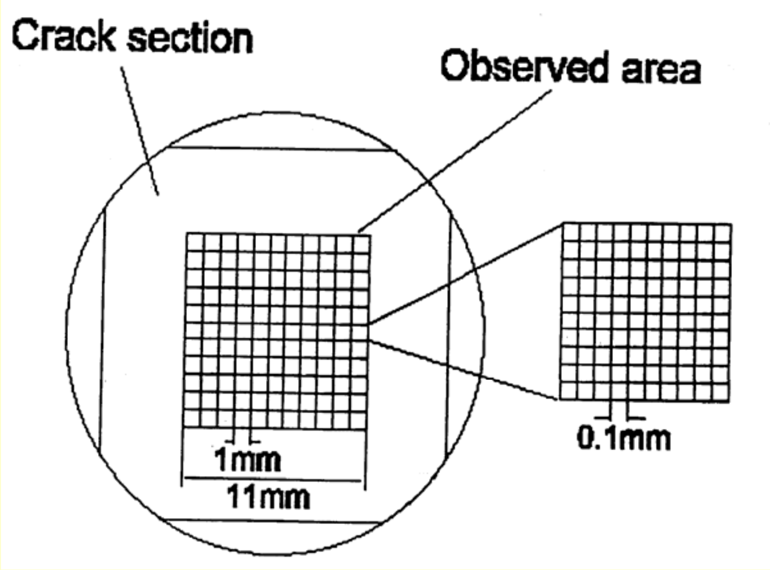

Crack Intercept Density (P_L) :
perpendicular *parallel*

WB1 (*pre-peak*)

WB2 (*peak*)

WB3 (*post-peak*)

Crack Intercept Density (P_L) :
perpendicular *parallel*

WD1 (ε_1 = 1.7%)

WD2 (ε_1 = 4.0%)

WD3 (ε_1 = 9.5%)

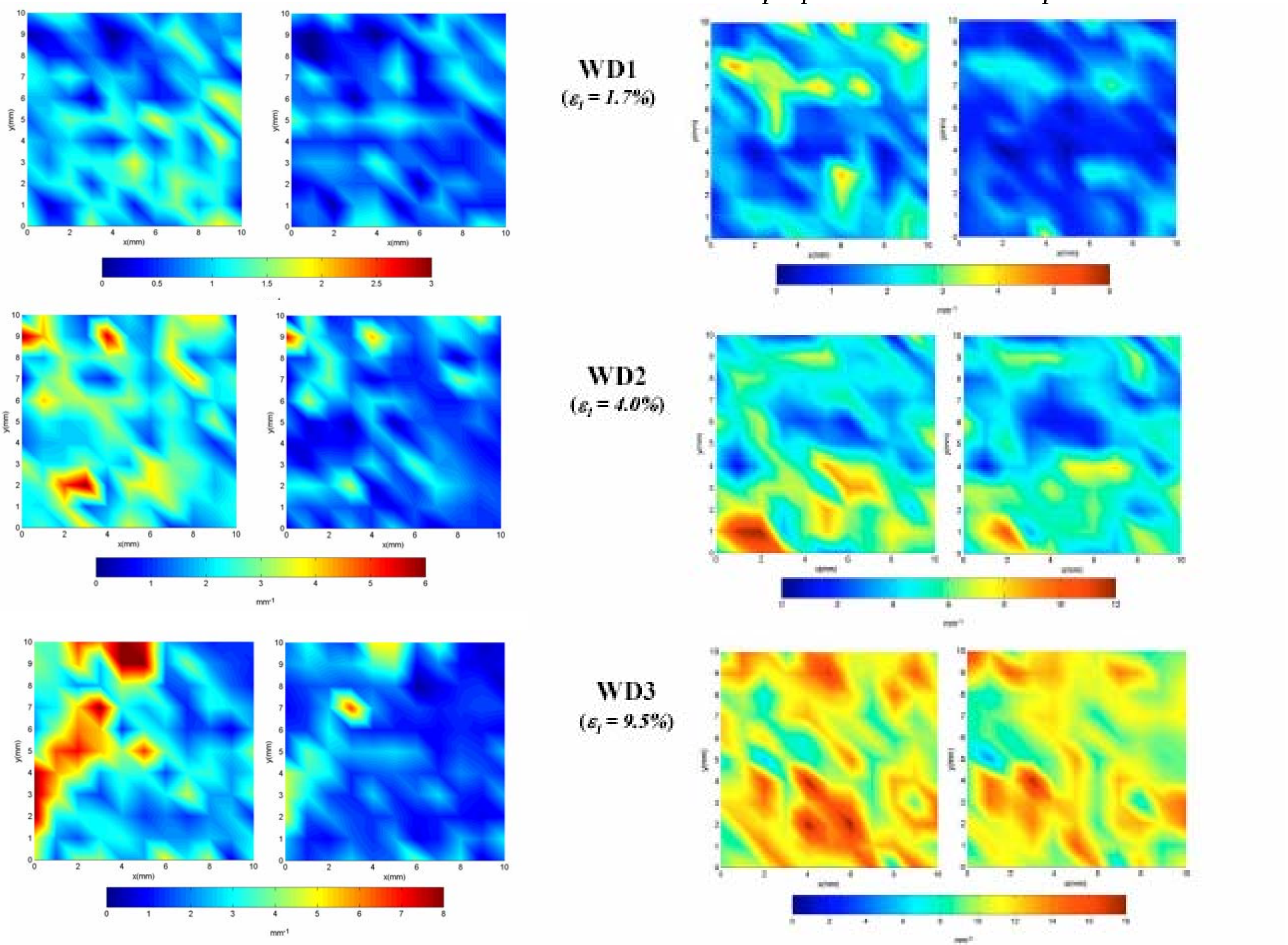

P_{eff} =10 MPa

Darley Dale sandstone (*Wu, Baud & Wong*, 2000)

P_{eff} =200 MPa

Shear band in a sample of Rothbach sandstone deformed in the brittle regime

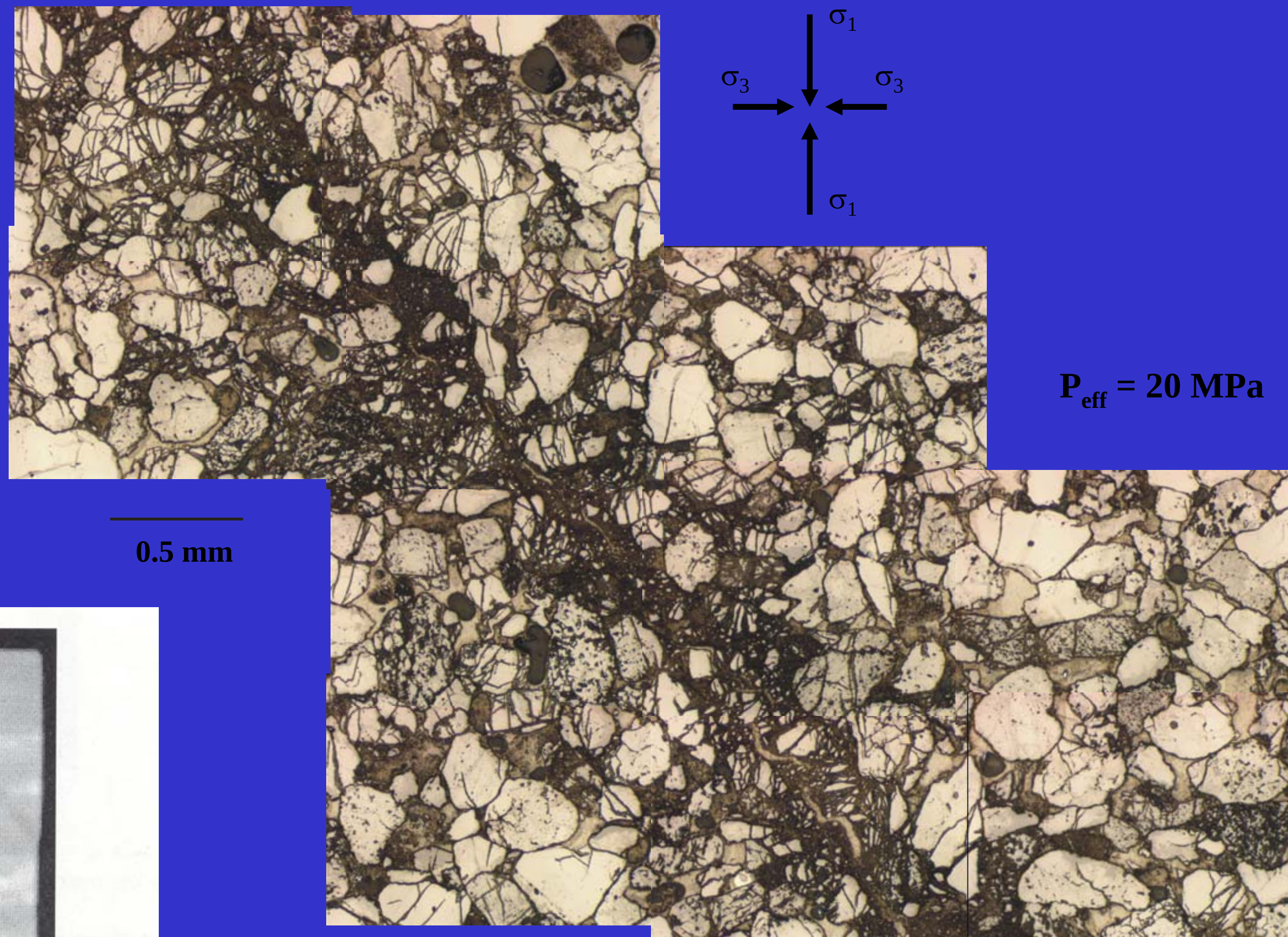

0.5 mm

P_{eff} = 20 MPa

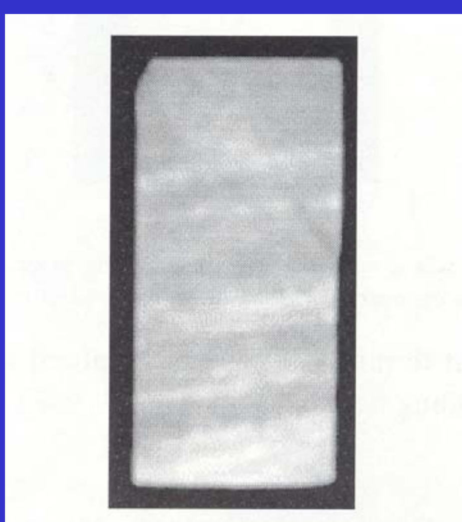

Bésuelle, Baud and Wong (2002)

Sample of Darley Dale sandstone deformed in the ductile regime

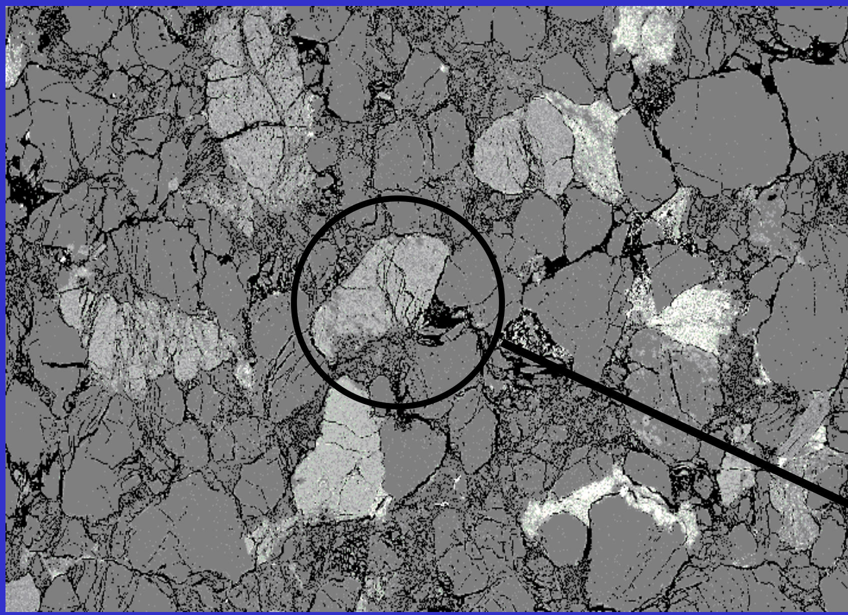

500 μm

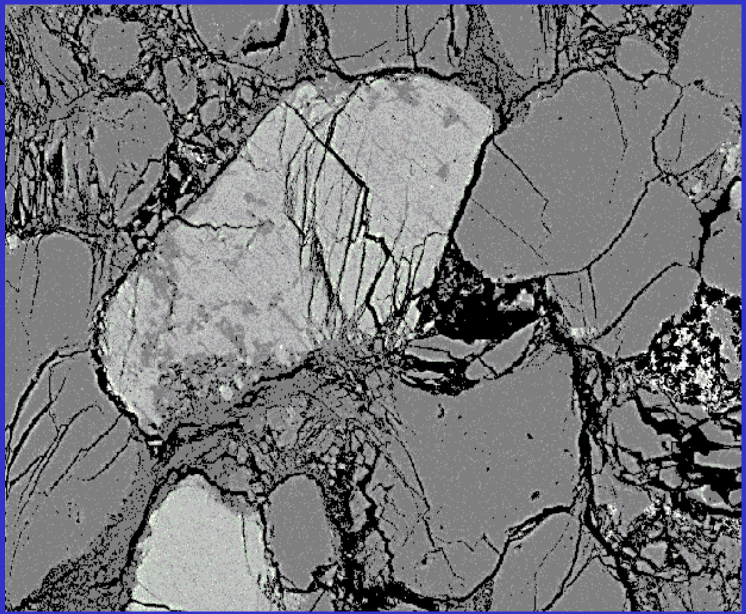

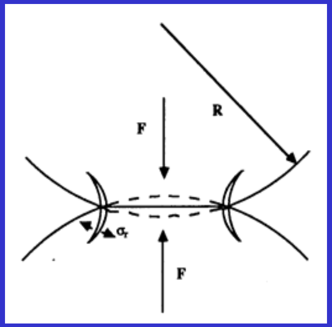

Hertzian fracture mechanics model

Wu, Baud and Wong (2000)

Damage Evolution and Acoustic Emission Activity

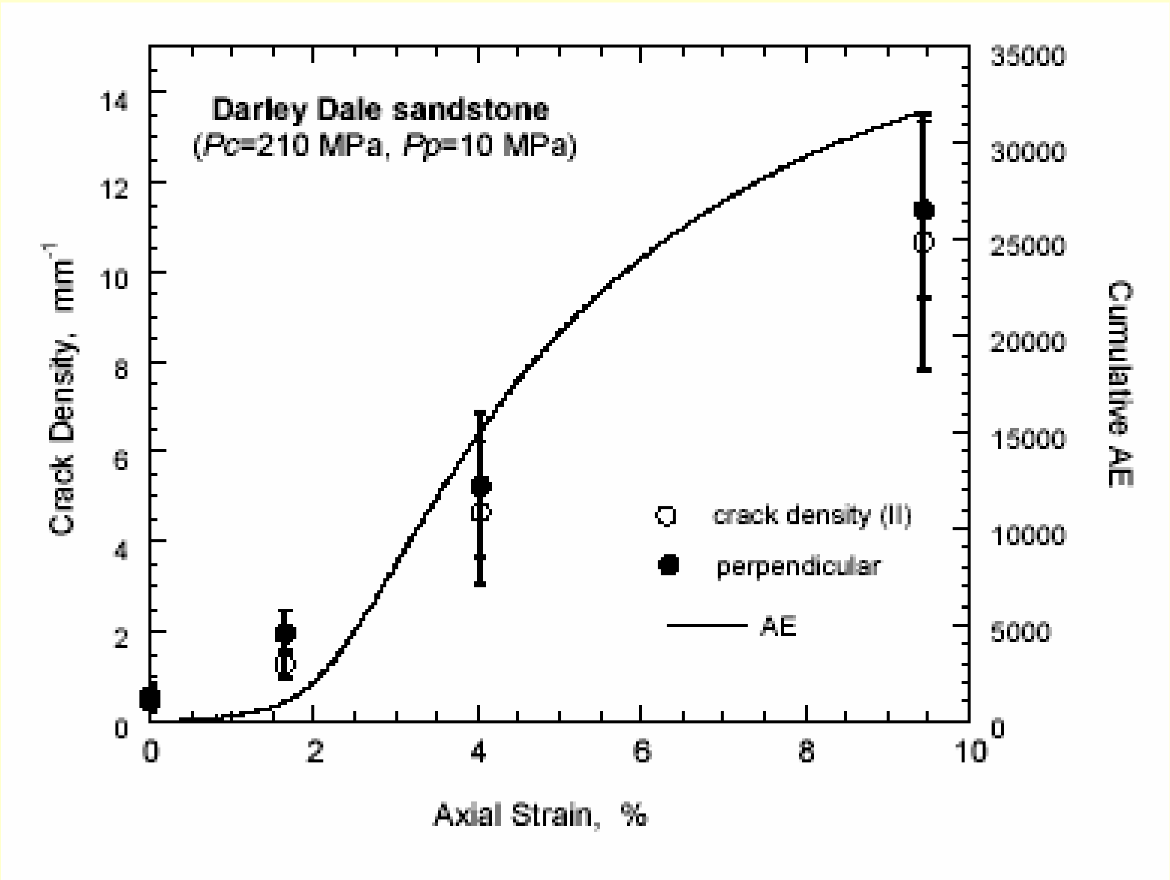

Wu, Baud & Wong (2000)

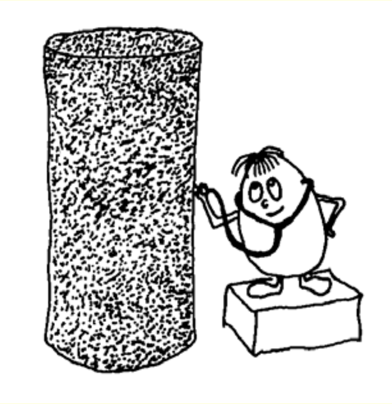

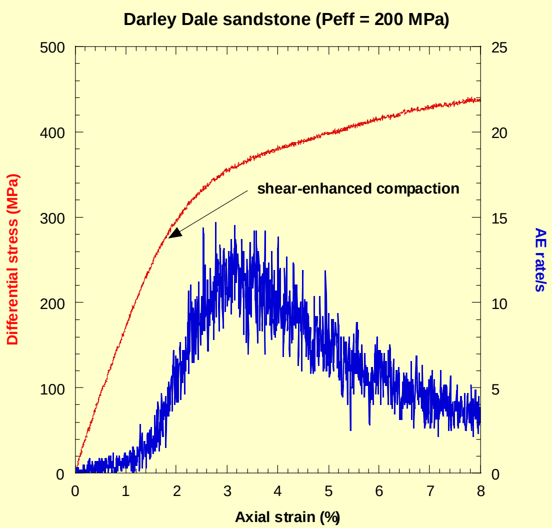

effective mean stress: $(\sigma_1+2\sigma_3)/3 - P_p$

P*: **grain crushing pressure**

C*: **onset of shear-enhanced compaction**

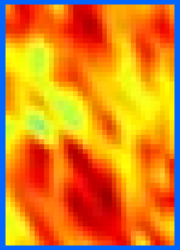

C': **onset of dilatancy**

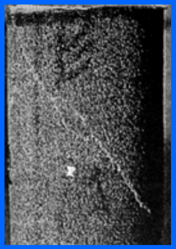

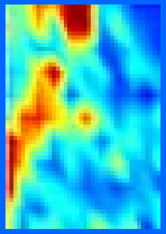

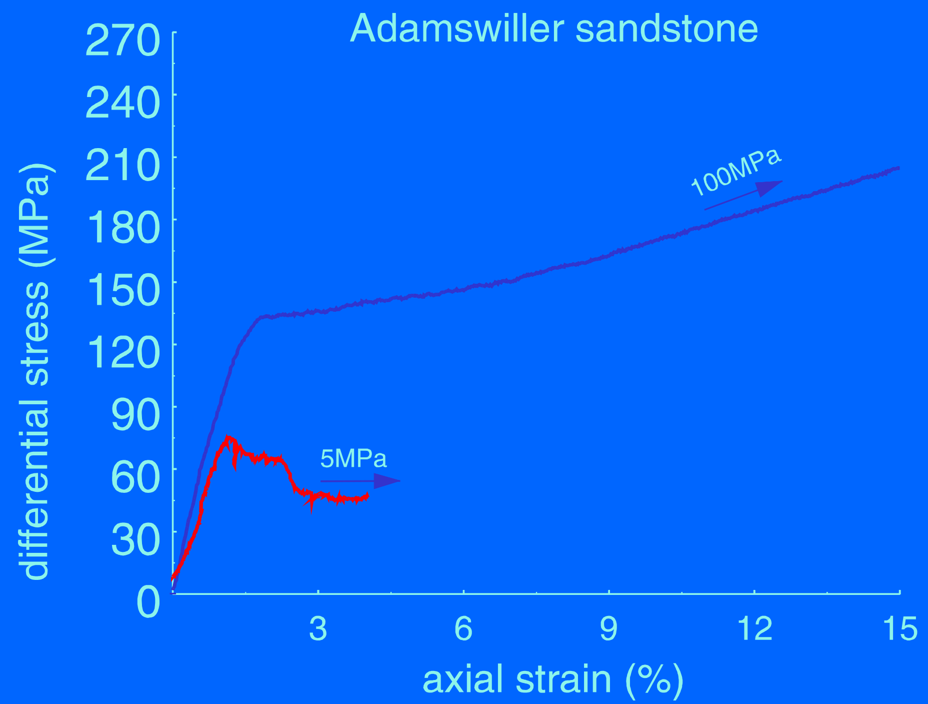

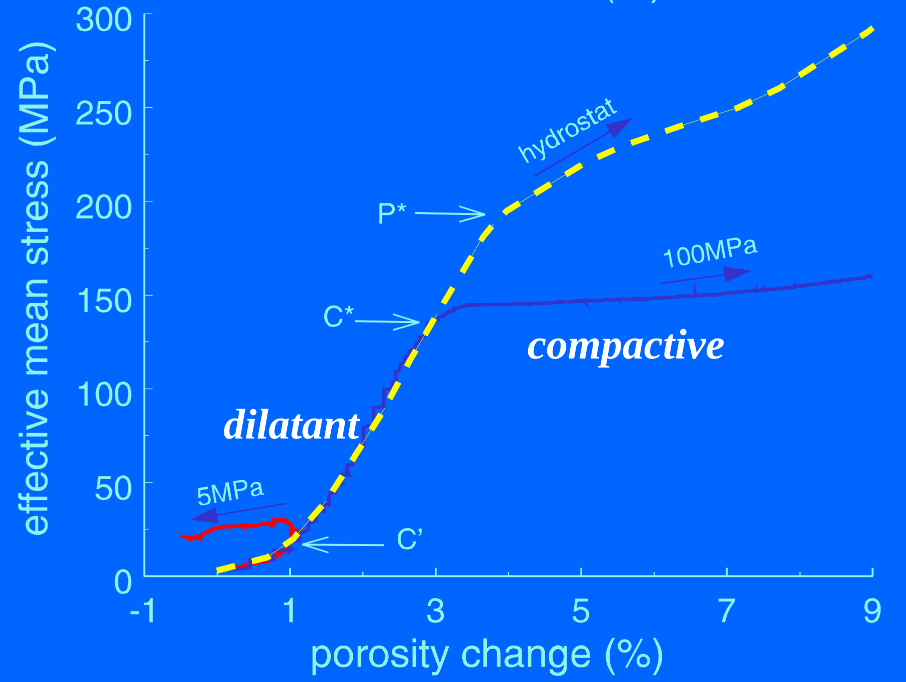

FAILURE MODES

brittle fracture:
shear localization

- ☞ *dilatancy*
- ☞ *low confinement*
- ☞ *high stress*

compactive yield: ***bulk failure***

- ☞ *shear-enhanced compaction*
- ☞ *high confinement*
- ☞ *low nonhydrostatic stress*

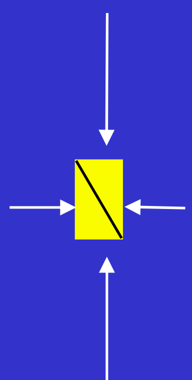

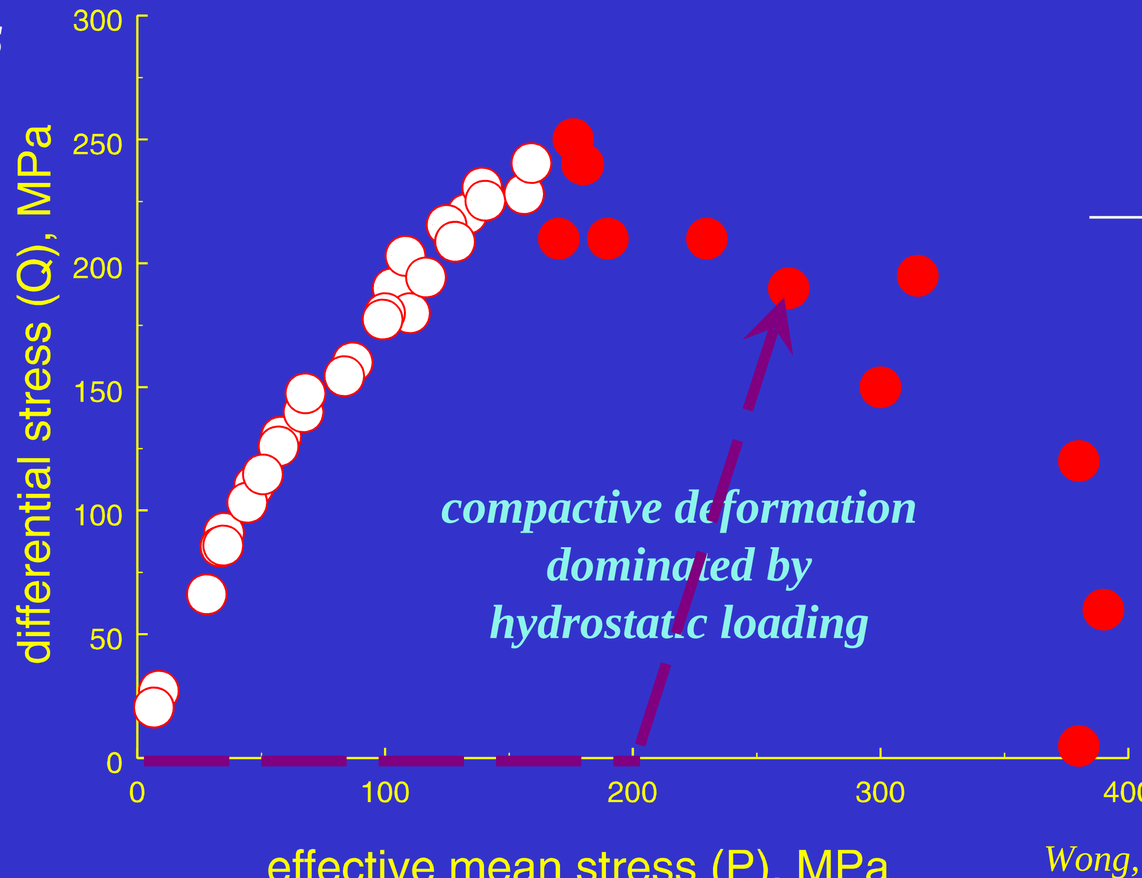

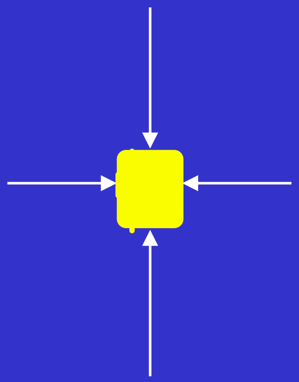

BEREA SANDSTONE

Wong, David and Zhu (1997)

II. Laboratory observations of compaction localization

→ Brittle-ductile transition ?

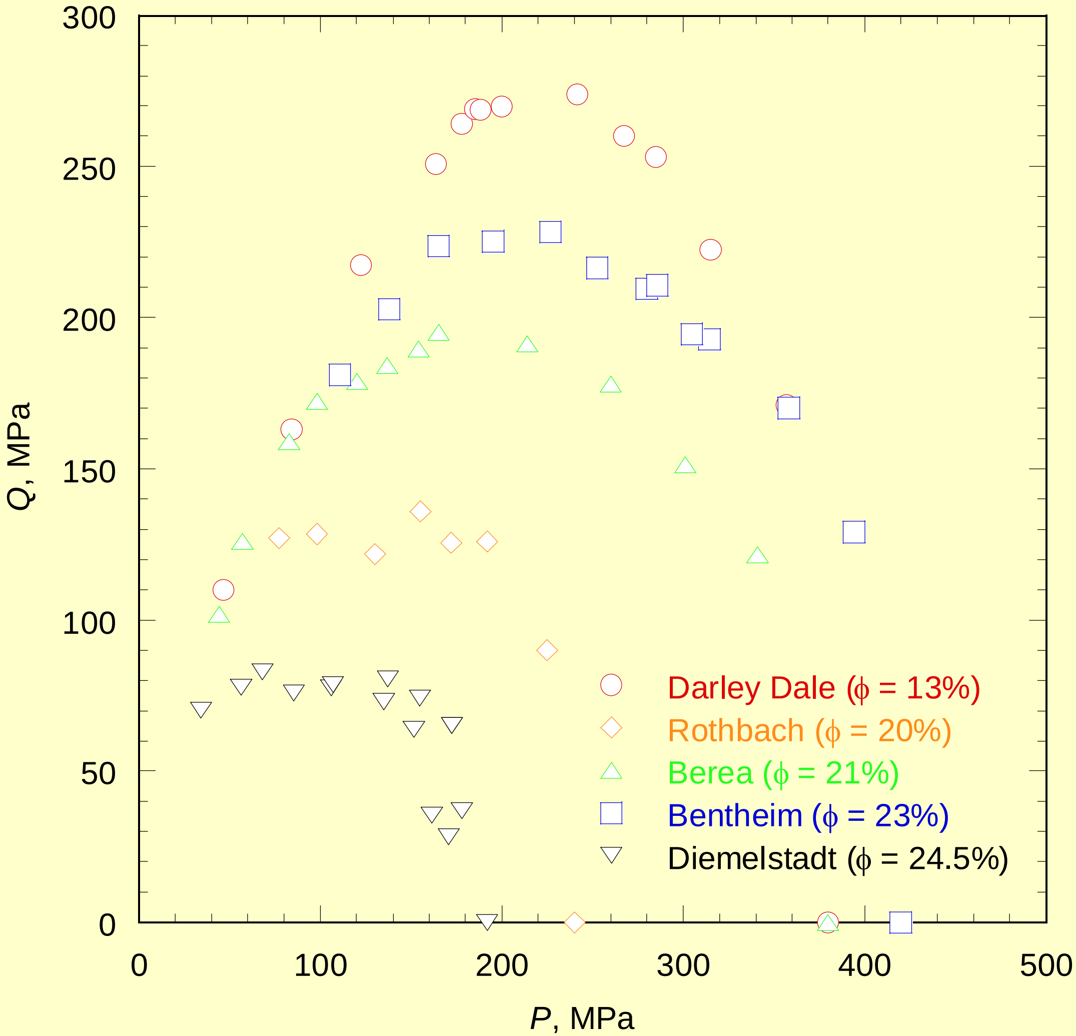

Darley Dale sandstone (ϕ = 13%)

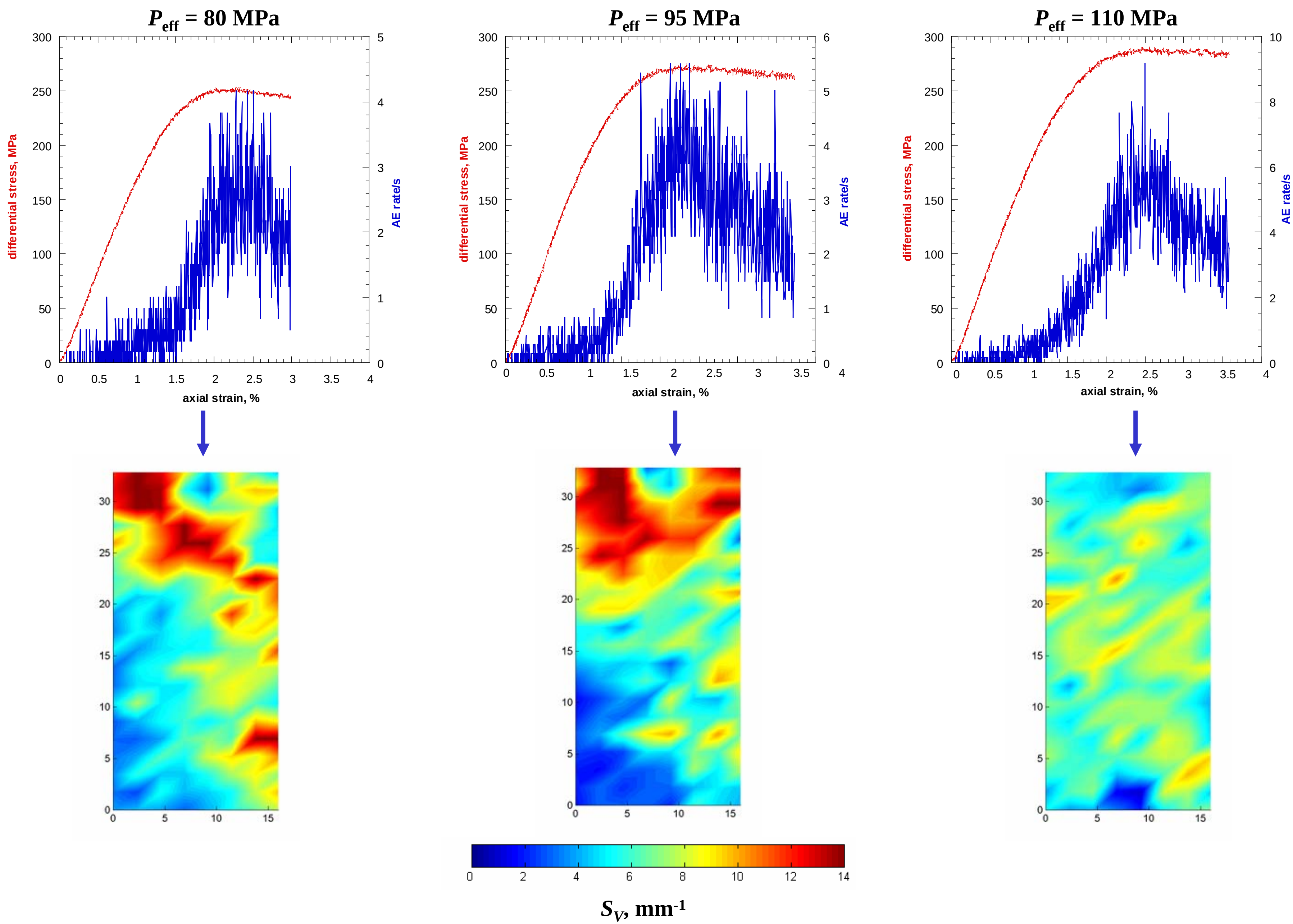

1. Conjugate shear bands

Compacting shear bands *(Bésuelle, 2001)*

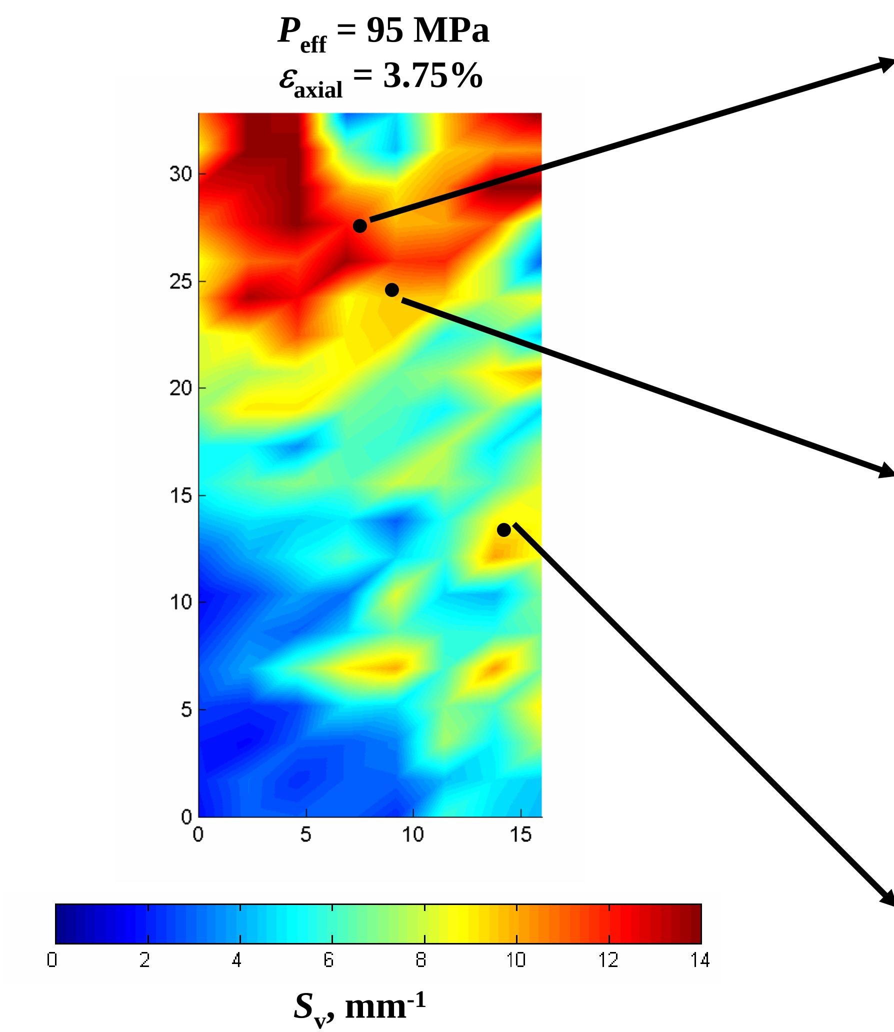

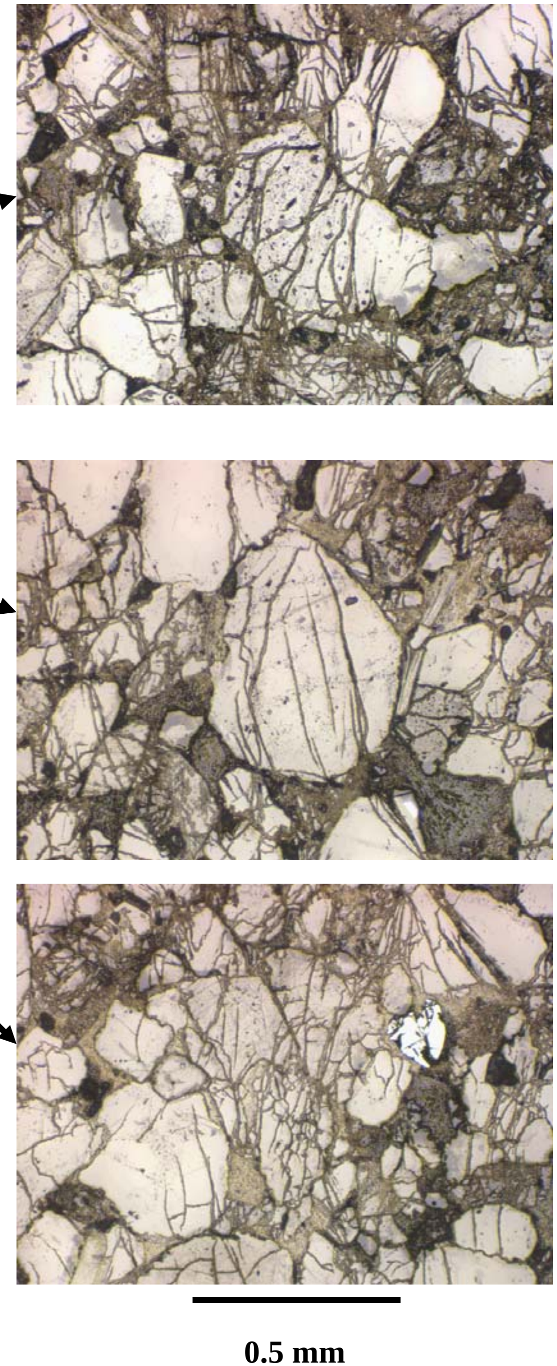

Darley Dale sandstone (ϕ = 13%)

Bentheim sandstone
(ϕ = 23 %)

confining pressure
120 MPa

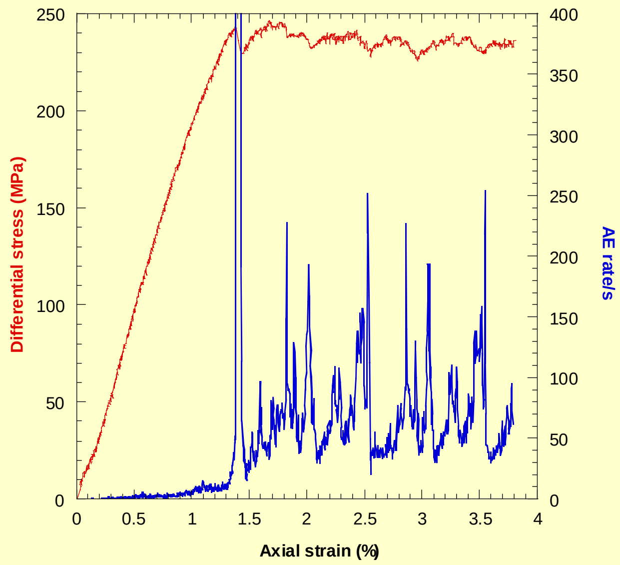

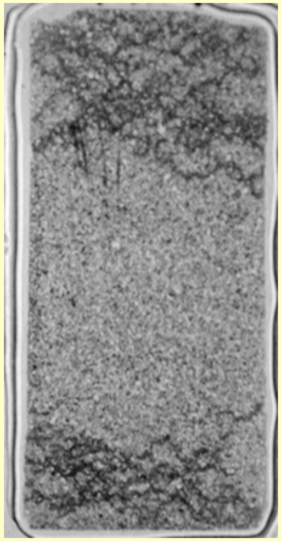

1 cm

300 MPa

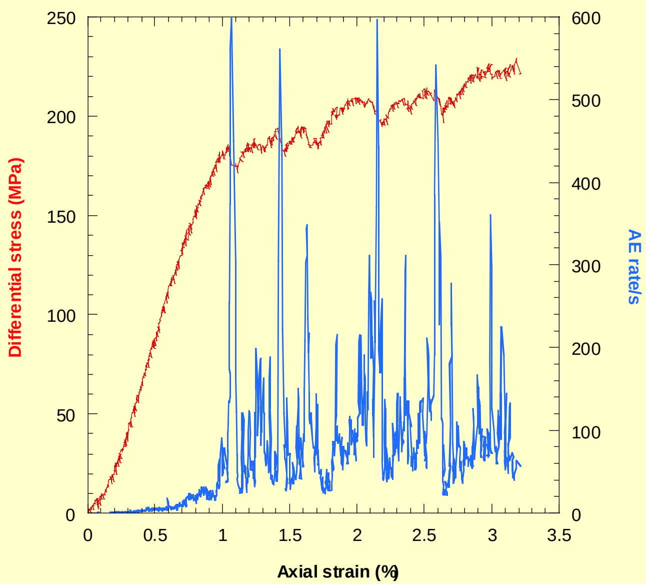

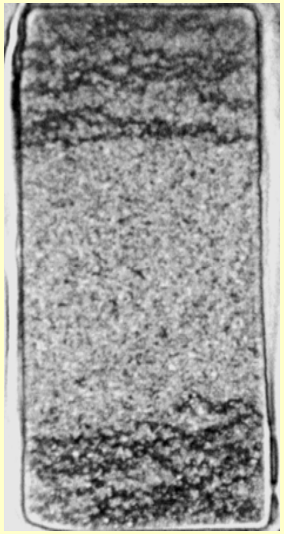

1 cm

2. *Discrete* compaction bands

Bentheim sandstone: Pc = 300 MPa

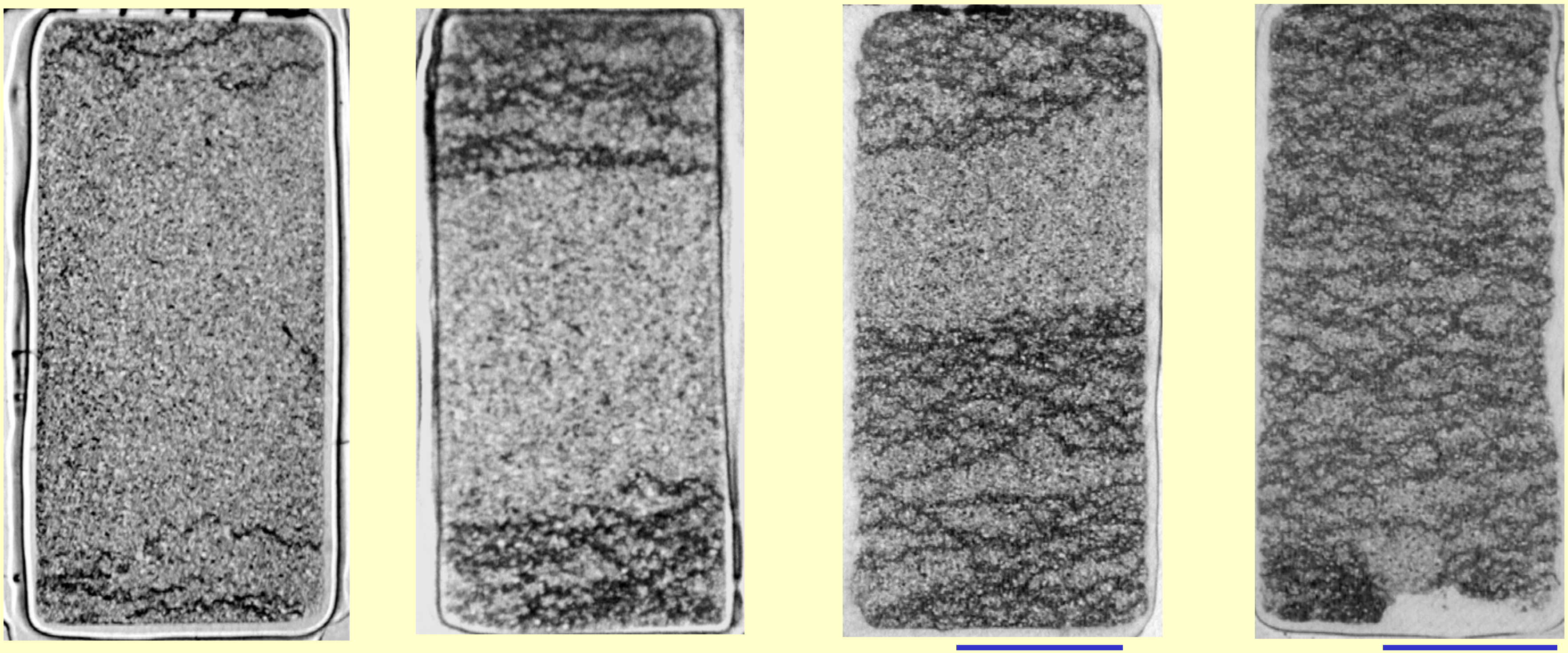

1 cm　1 cm　1 cm　1 cm

$\varepsilon_{ax} = 1.4$ %　$\varepsilon_{ax} = 3.1$ %　$\varepsilon_{ax} = 4$ %　$\varepsilon_{ax} = 6$ %

Baud, Klein and Wong (2004)

A compaction band in the Bentheim sandstone: typically the lateral width extends over 2 grains or so (~ 600 μm)

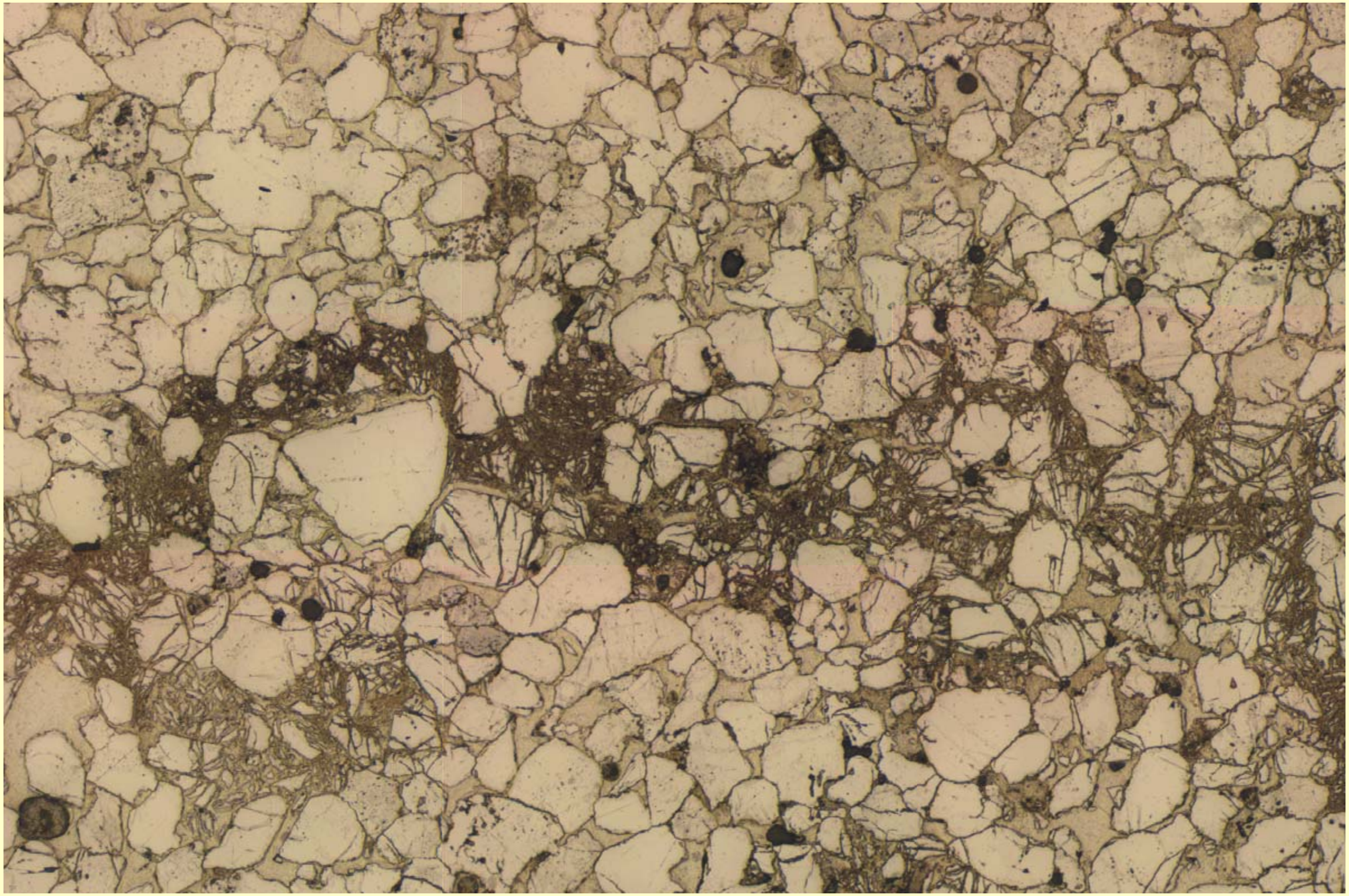

0.5 mm

Baud, Klein and Wong (2004)

Tortuous compaction band in Diemelstadt sandstone ($\phi = 25\%$)

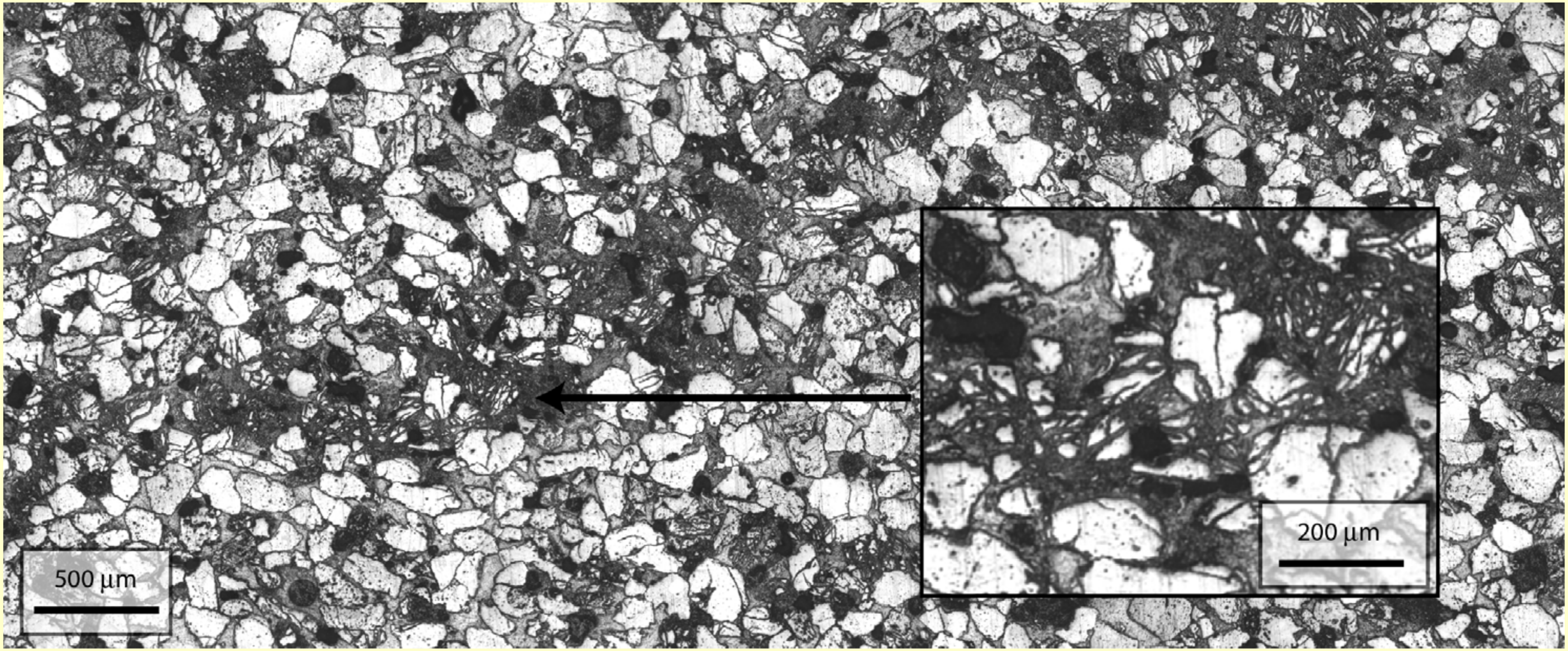

Tembe et al. (in preparation)

Conjugate shear bands **(Berea sandstone, ϕ = 21%)**

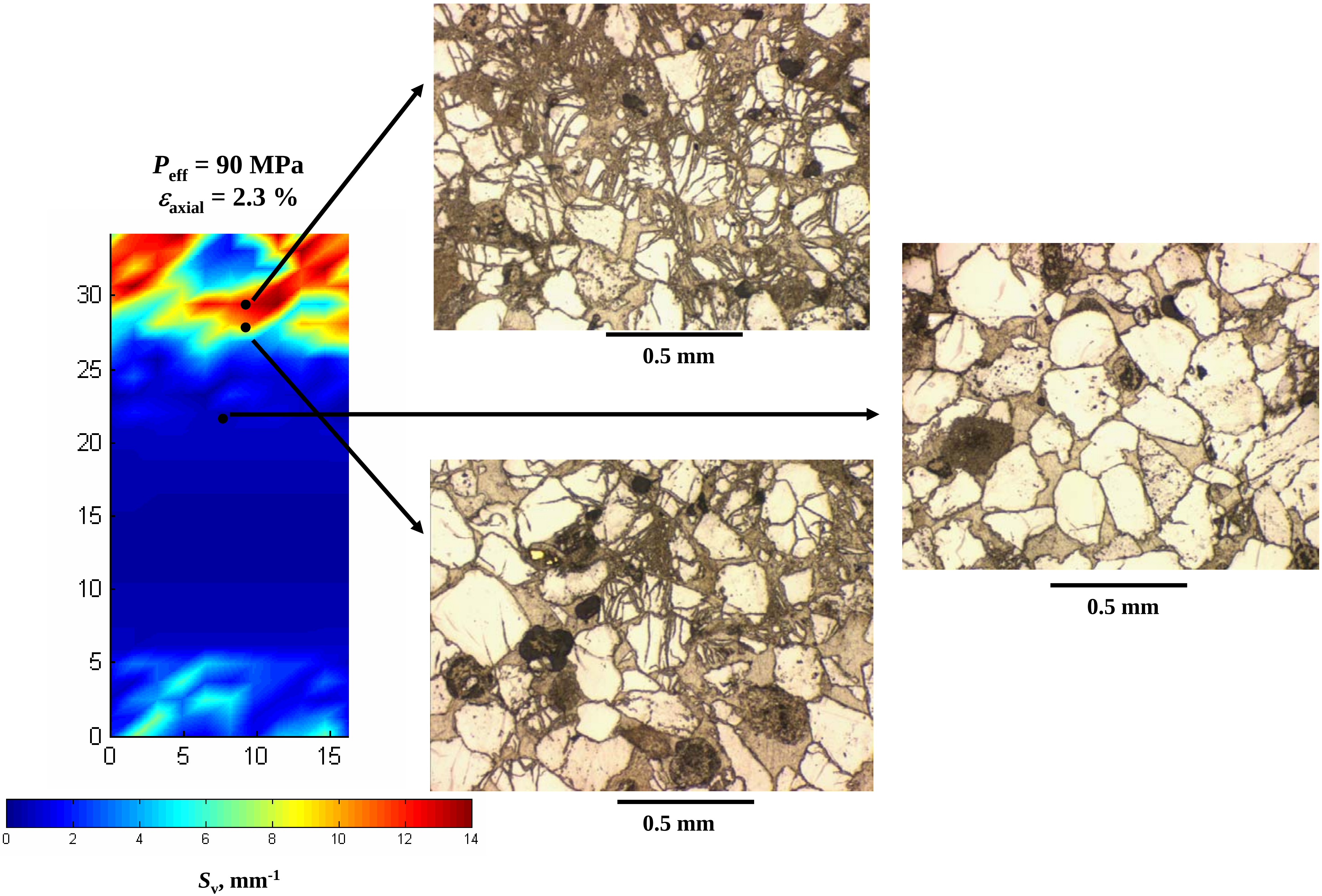

Berea sandstone, $\phi = 21\%$

P_{eff} = 200 MPa
ε_{axial} = 3.2 %

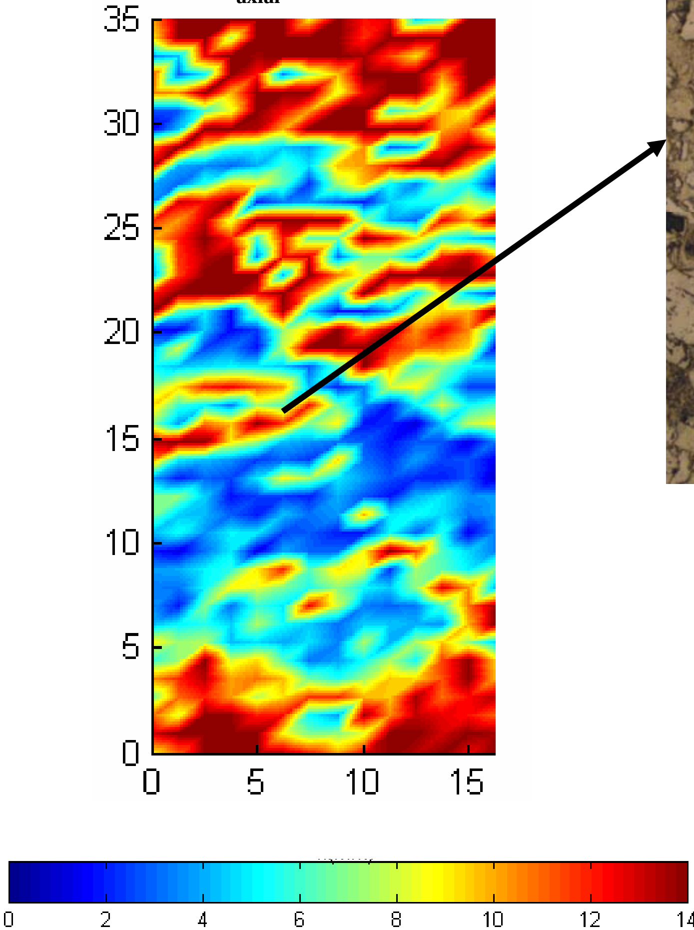

S_v, mm^{-1}

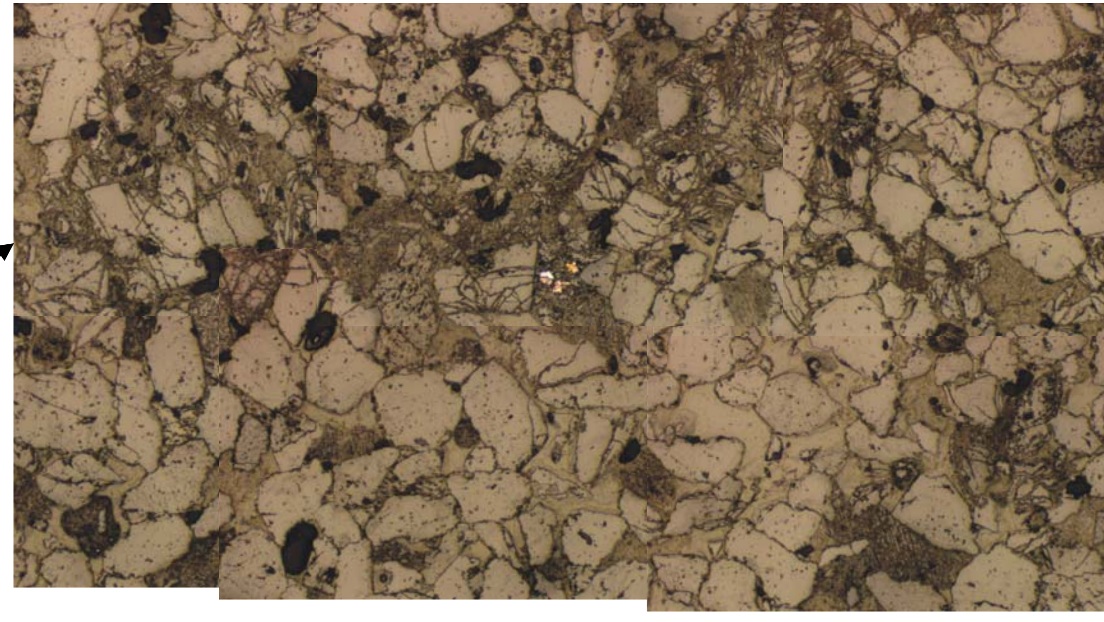

0.5 mm

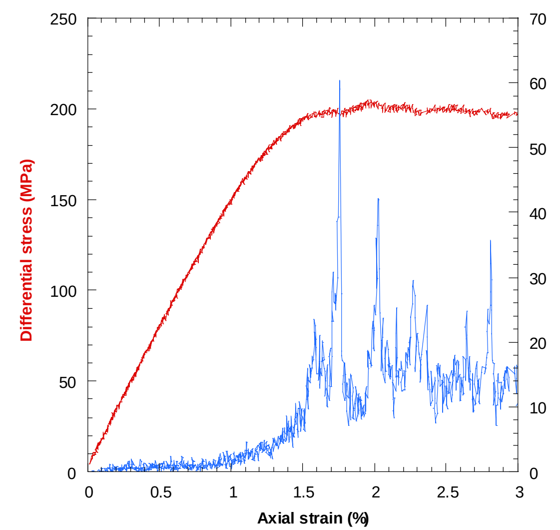

3. *Diffuse* compaction bands

P_{eff} = 130 MPa
ε_{axial} = 3.6%

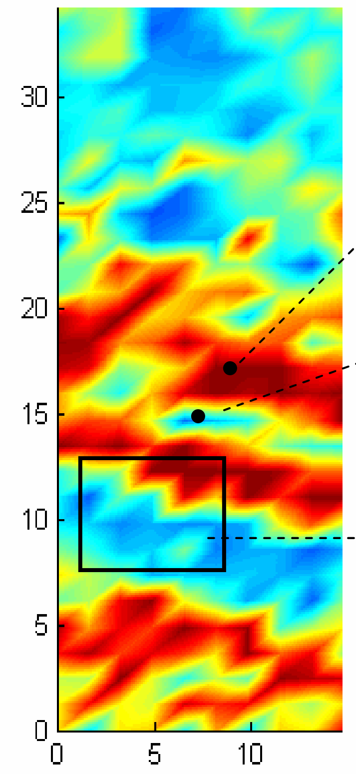

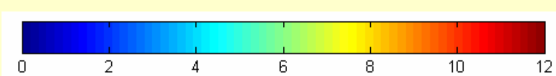

mm^{-1}

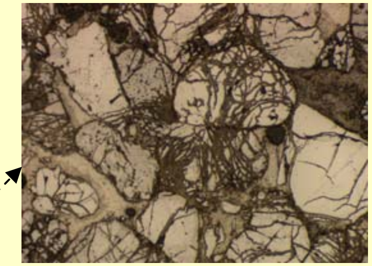

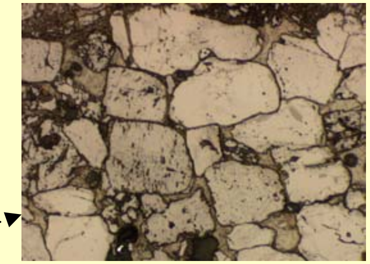

0.5 mm

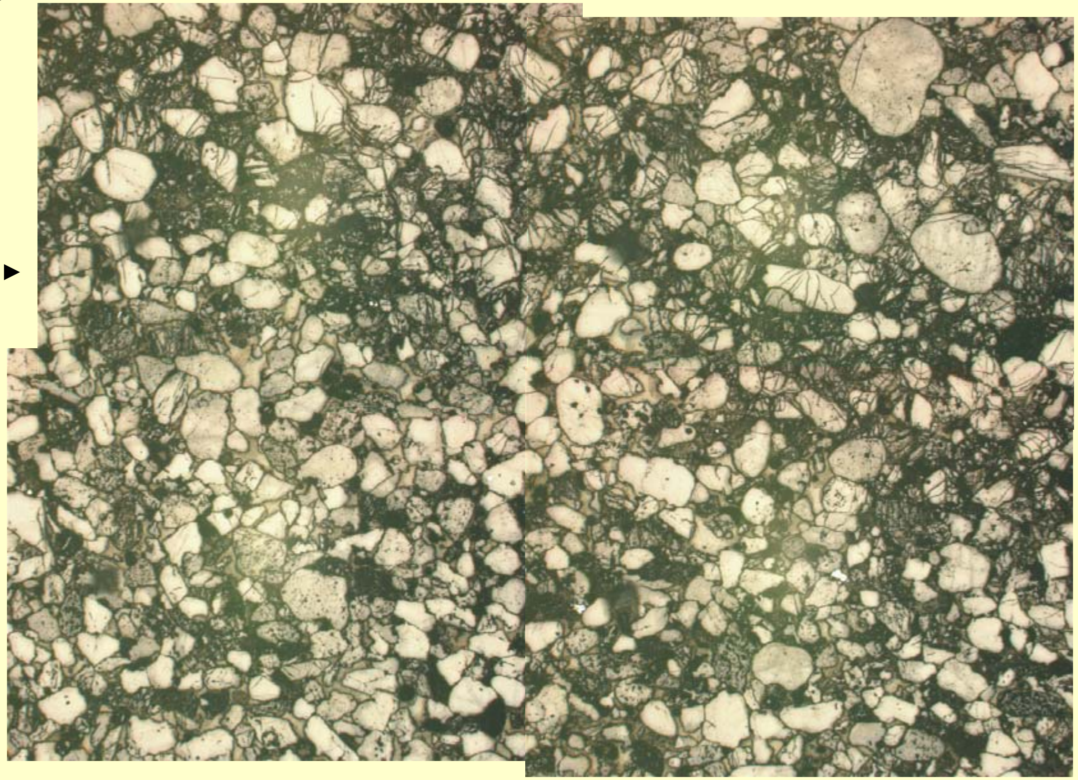

1 mm

Rothbach sandstone
(ϕ = 20%)

Bésuelle, Baud and Wong (2002)

ACOUSTIC EMISSION LOCATION

Discrete compaction bands in Bleurwiller sandstone ($\phi = 25\%$)

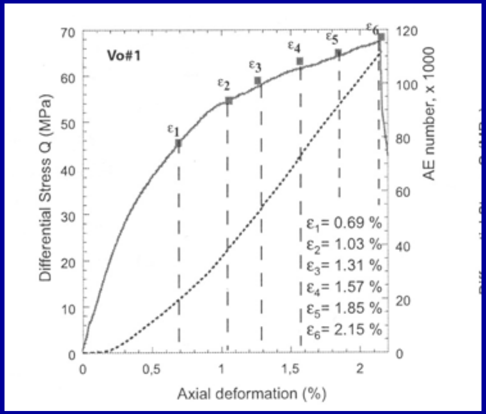

Diffuse compaction bands in Castlegate sandstone ($\phi = 28\%$)

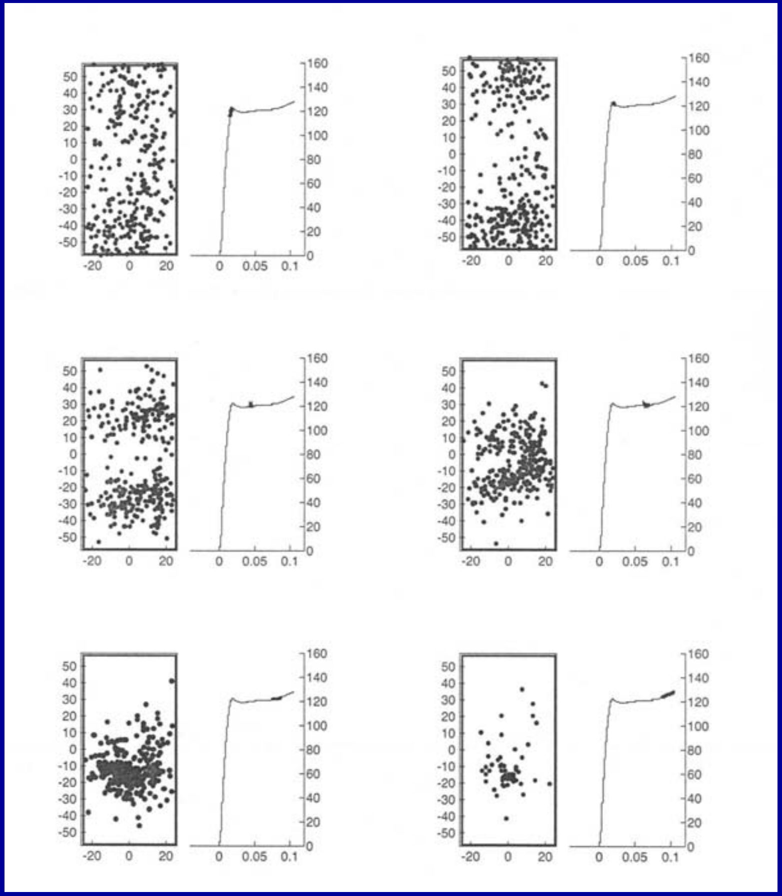

Olsson and Holcomb (2000)

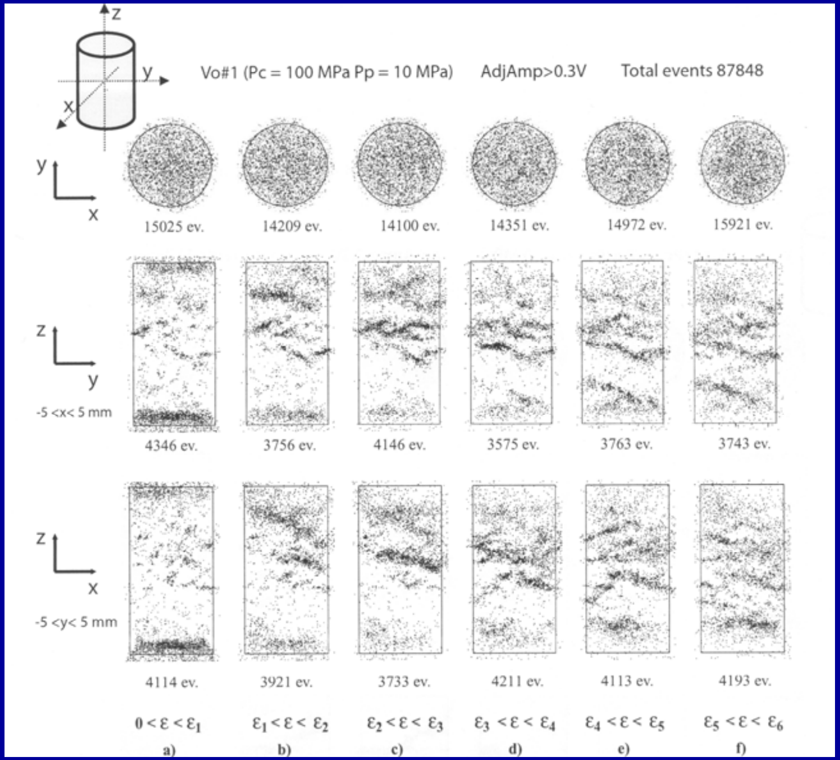

Fortin et al. (submitted)

Summary of failure modes

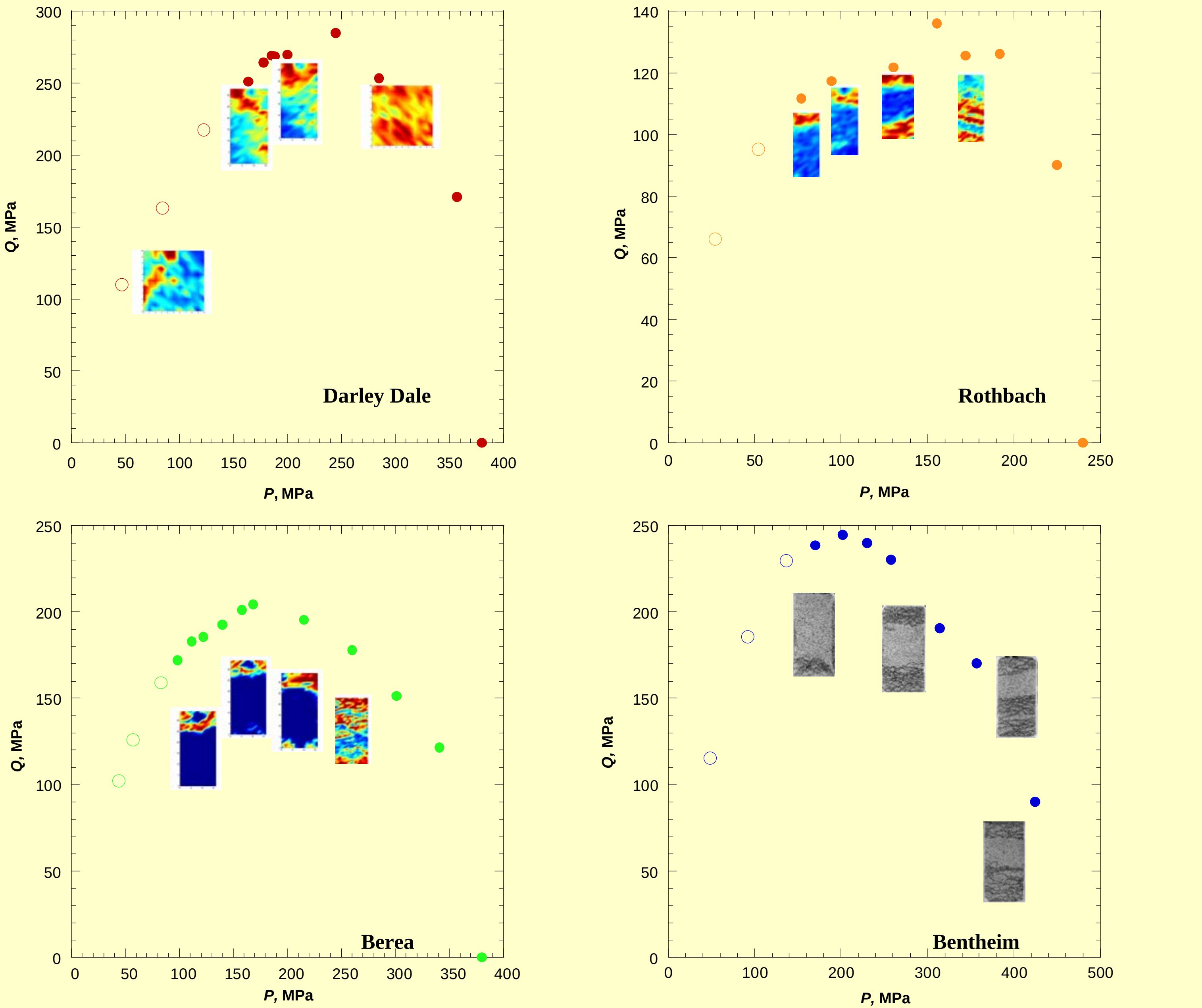

Baud et al., JSG (2004)

Compaction

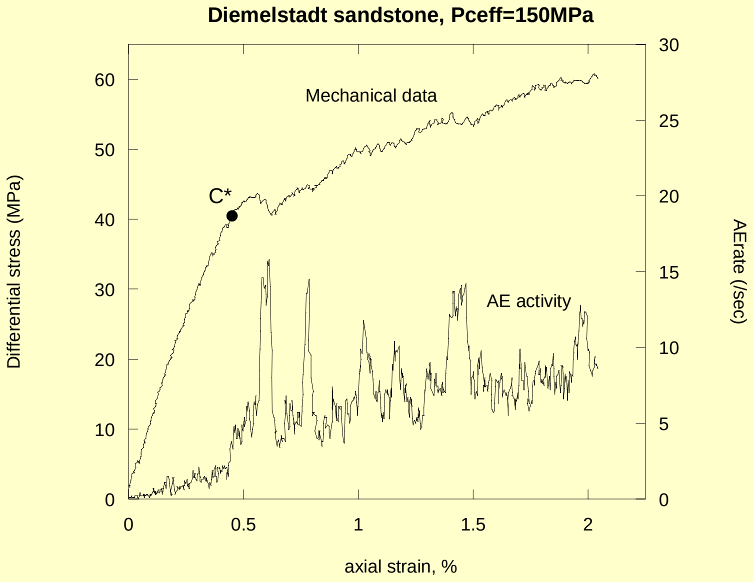

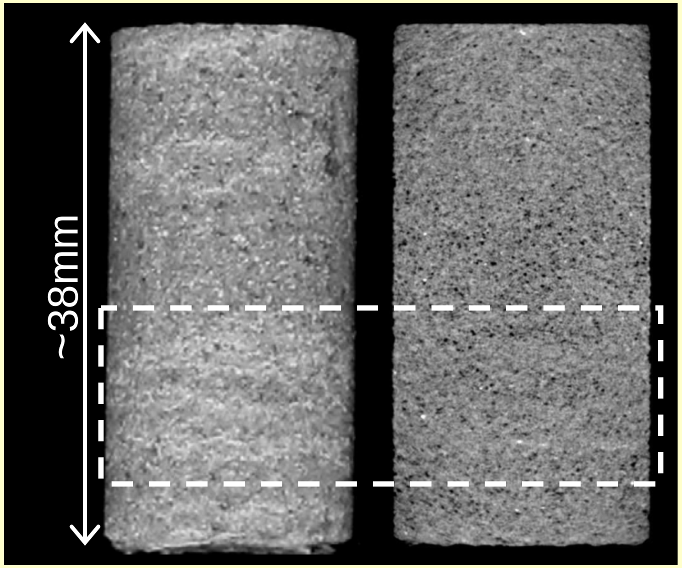

X-ray CT imaging

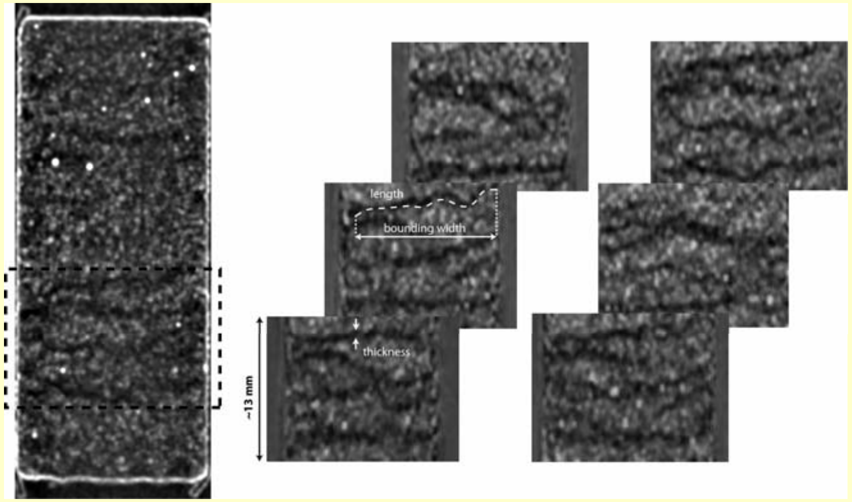

→ **compaction bands: $\Delta\phi \sim 15\%$**

Wong, Louis, and Baud (submitted)

Post-yielding porosity reduction: compaction bands versus homogeneous cataclastic flow

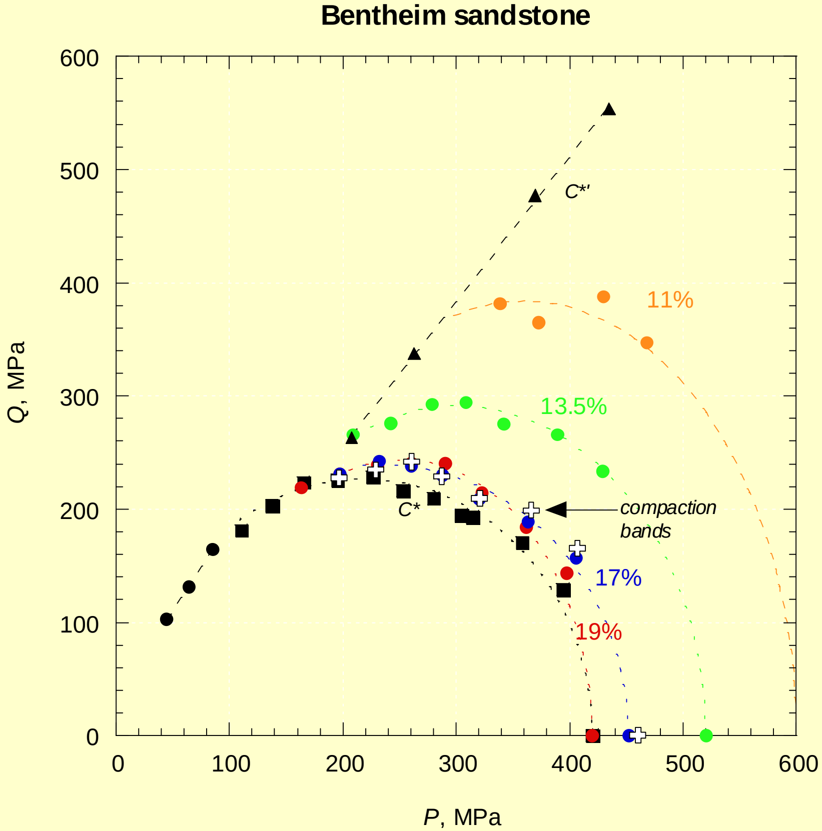

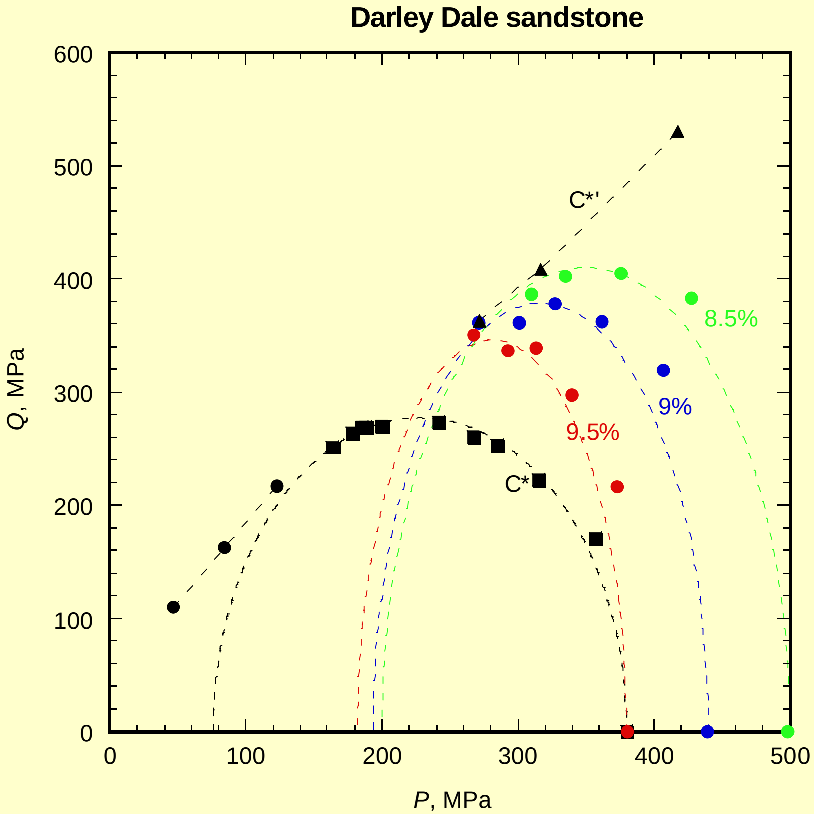

Baud, Vajdova, and Wong (submitted)

Plastic volumetric strain: elliptical contours

$$\frac{(P-C)^2}{A^2}+\frac{Q^2}{B^2}=1$$

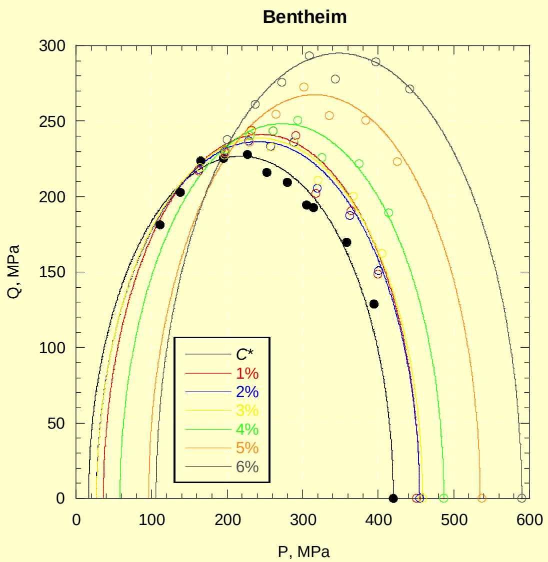

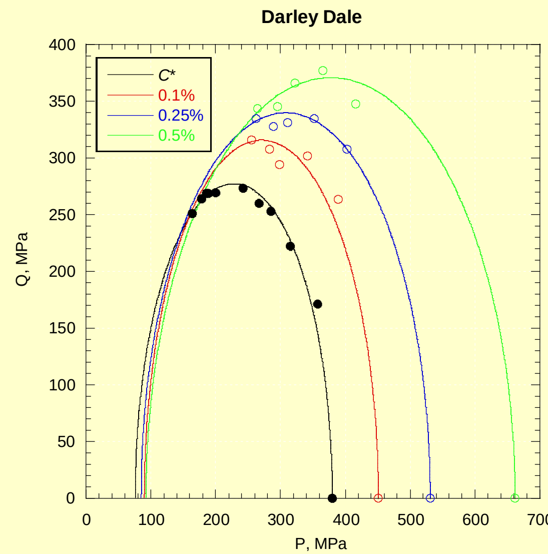

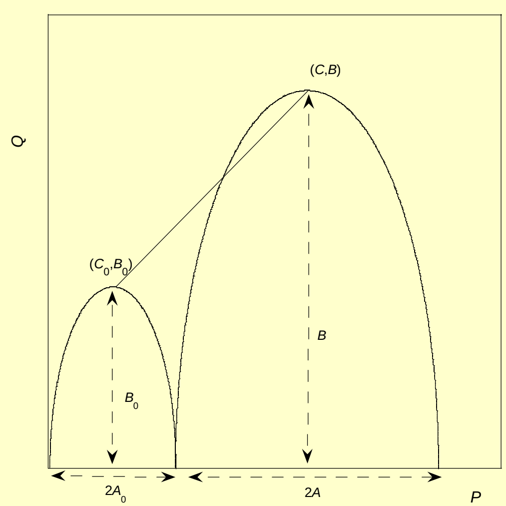

- compaction bands:

  $B/A \sim \text{cte}$

- homogeneous cataclastic flow:

  $B/A \downarrow$ with plastic strain

IV. Influence on fluid flow

Experimental set-up (*Zhu and Wong, 1997*)

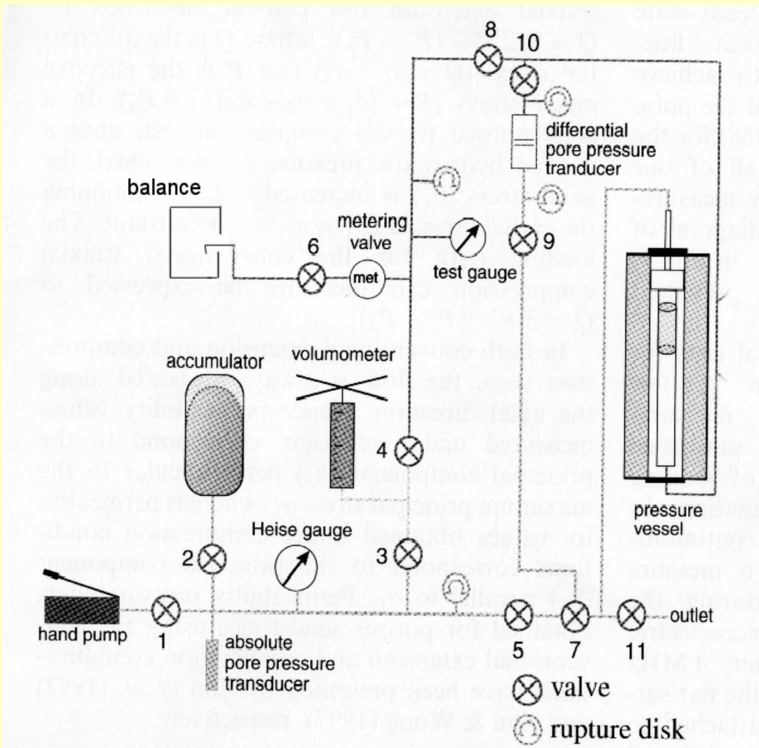

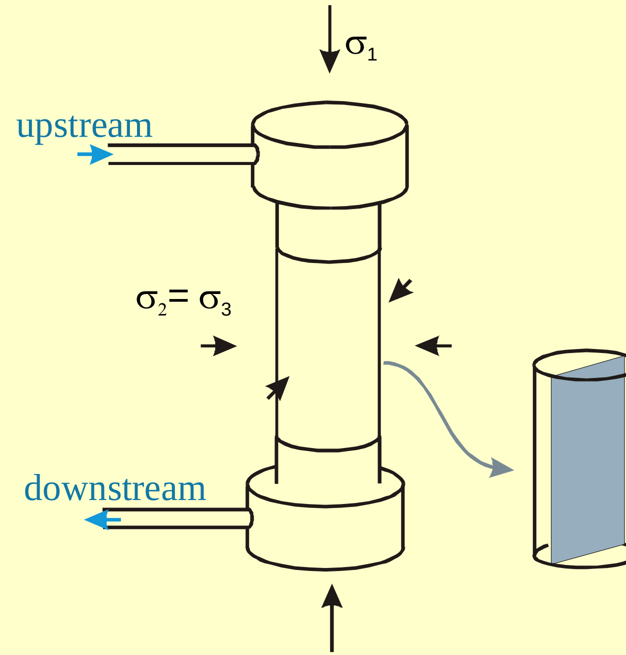

- conventional triaxial experiment with stops for permeability measurements
- water flow in direction of σ_1, steady-state flow technique
- microstructural observations on failed samples performed on thin section

Permeability evolution in Bentheim sandstone ($\phi = 23\%$)

shear
localization

$P_{eff} = 10$ MPa

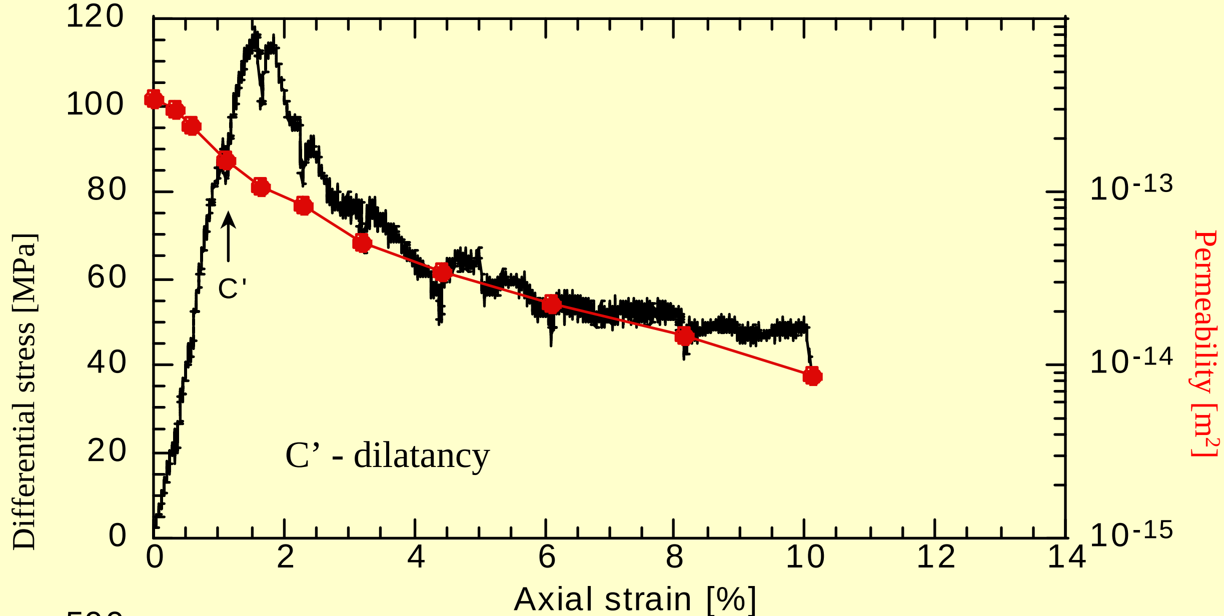

compaction
localization

$P_{eff} = 300$ MPa

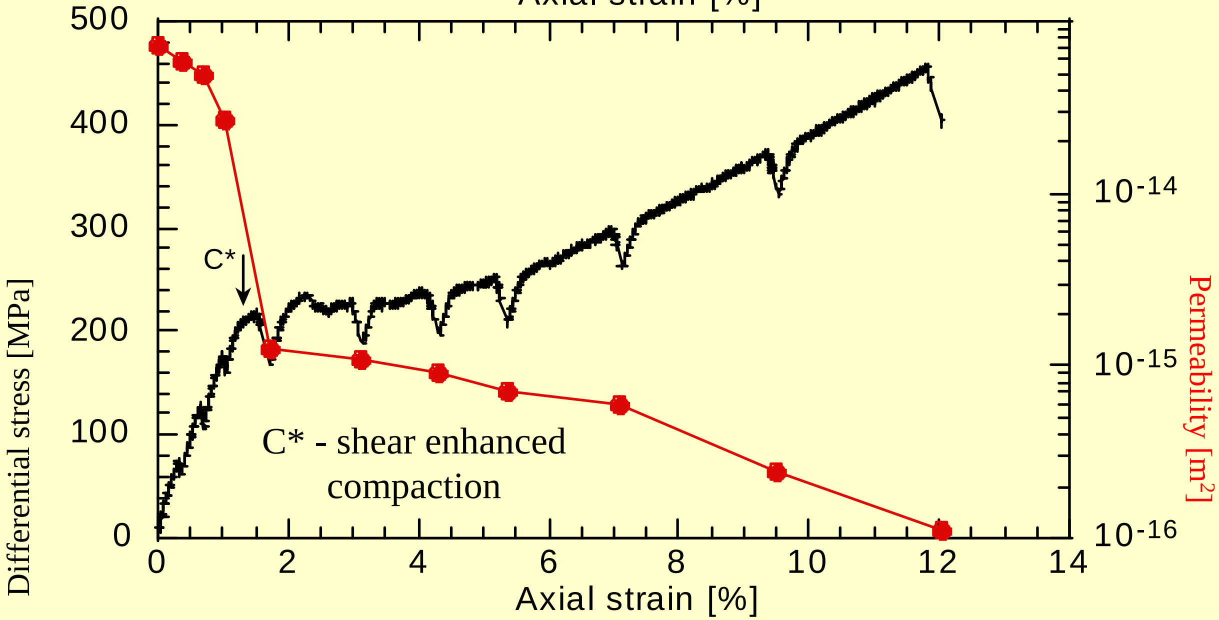

Vajdova, Baud, and Wong, JGR (2004)

Coupling of compaction band formation and permeability reduction

P_{eff} =250 MPa

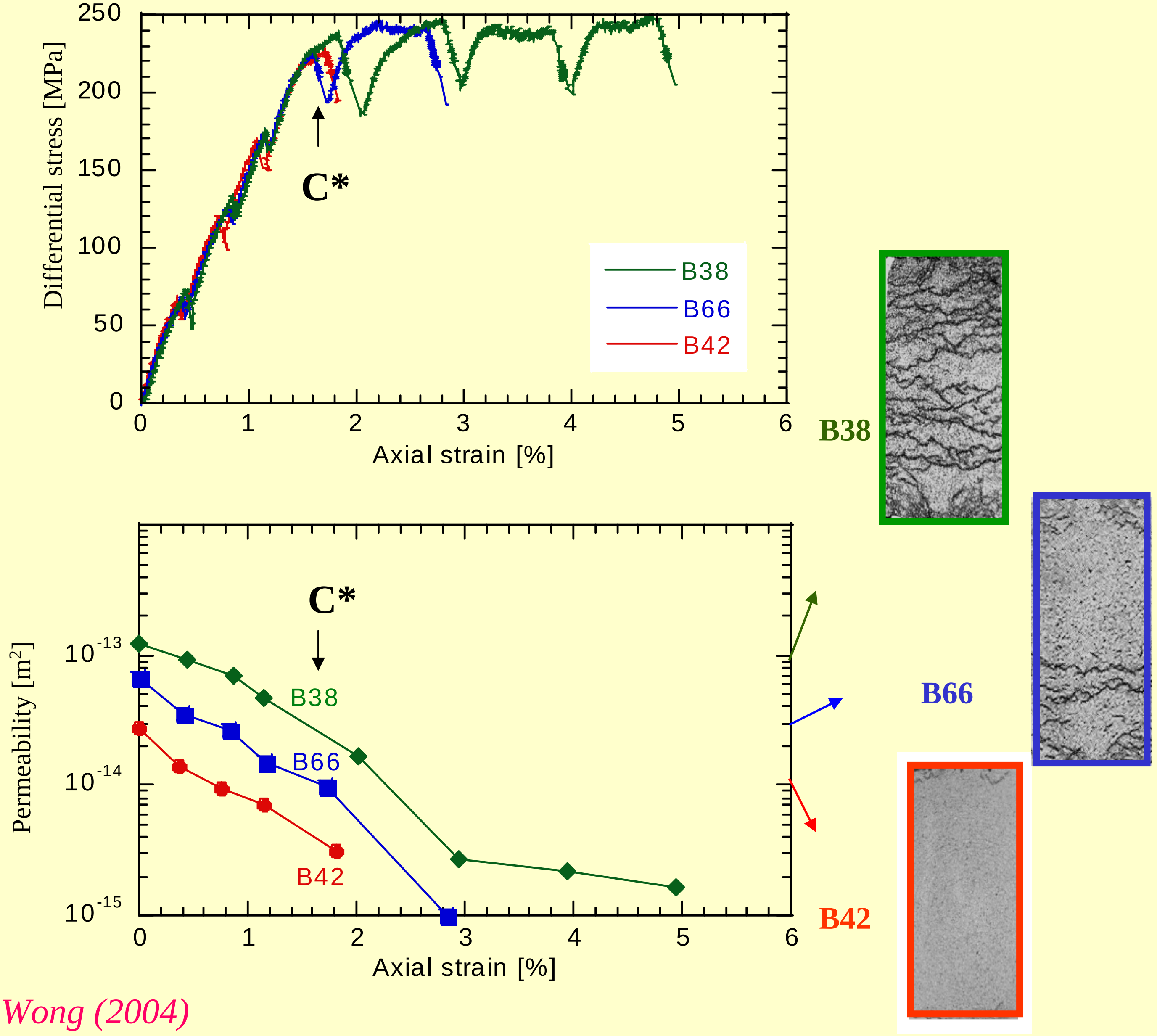

Vajdova, Baud and Wong (2004)

Number of compaction bands as a function of plastic strain

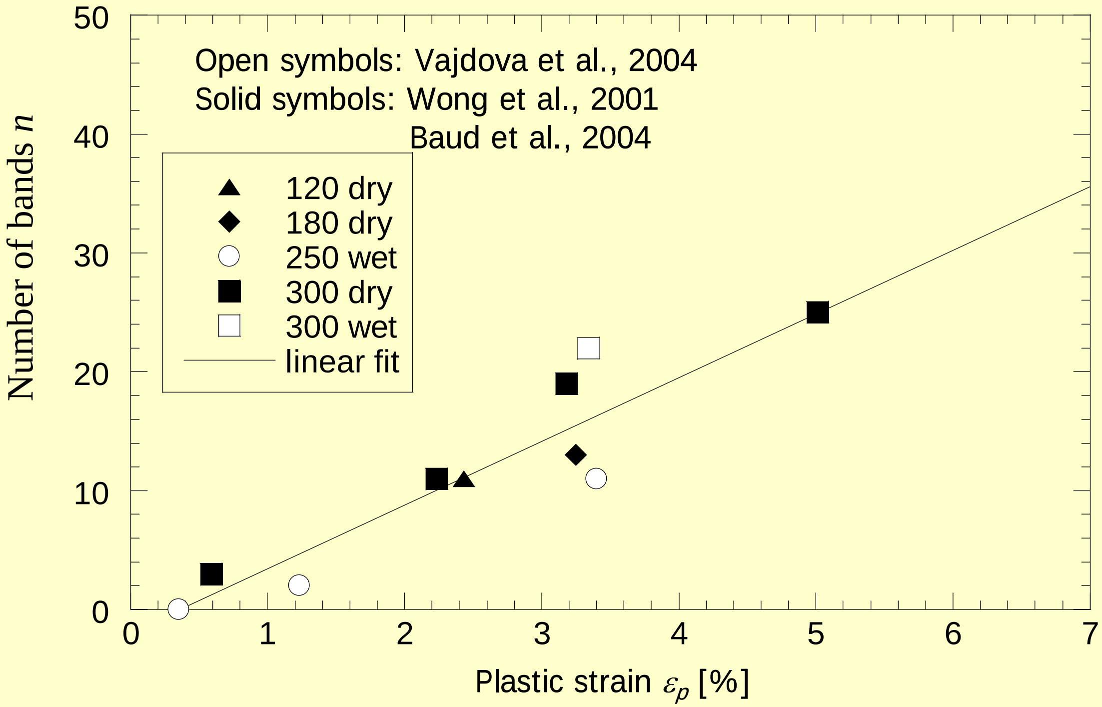

$$\varepsilon_P = \varepsilon_0 + \beta \cdot n$$

$\varepsilon_0 = 0.00336$

$\beta = 0.00185$

Implications:

• compaction band formation is initiated only when plastic strain of $\varepsilon_0 = 0.336\%$ is achieved after the onset of shear-enhanced compaction C*

• development of each compaction band is associated with nominal plastic strain of $\beta = 0.185\%$

Permeability of a layered medium: a model for permeability evolution during compaction band formation

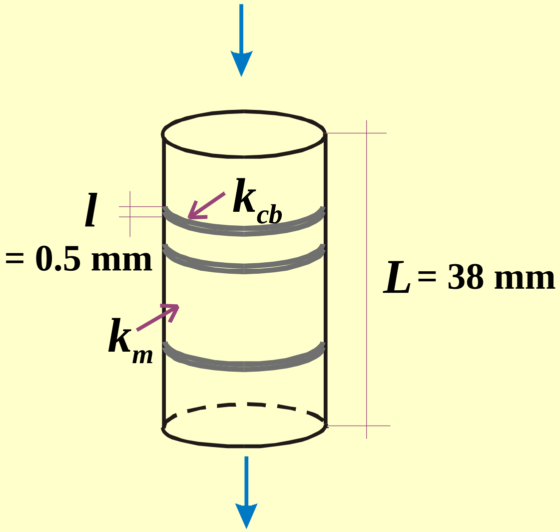

k_m/k_{cb} permeability contrast

$$k_{eff} = \frac{k_m}{\left(\frac{nl}{L}\right)\left(\frac{k_m}{k_{cb}} - 1\right) + 1}$$

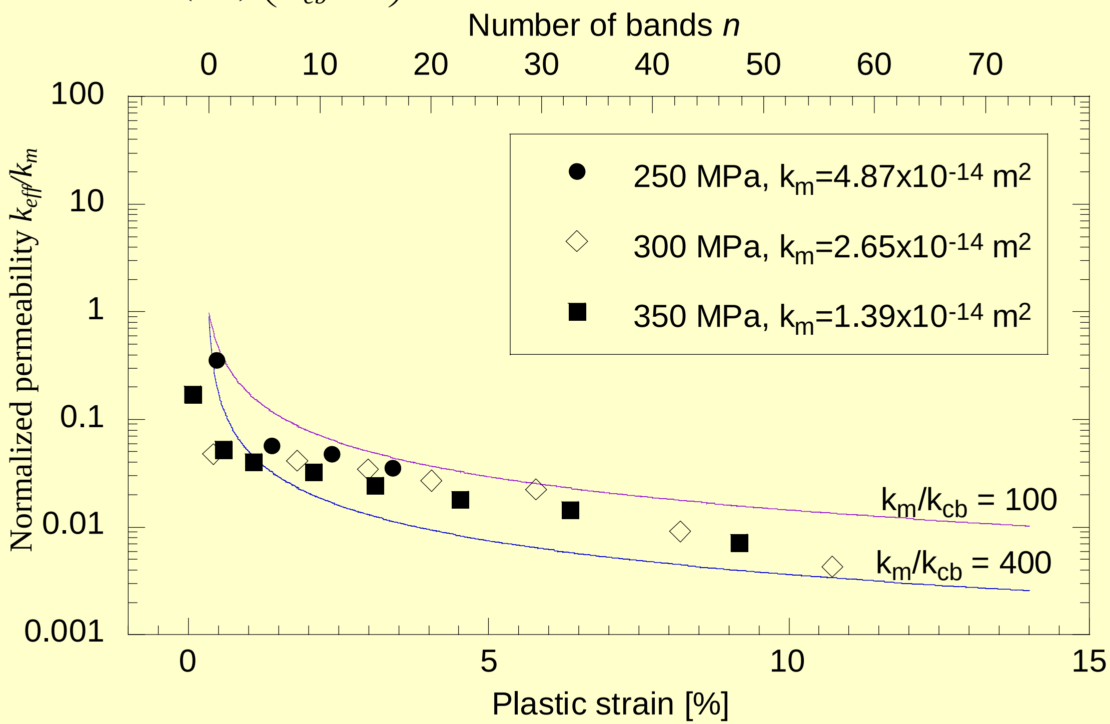

Implications:

- the permeability contrast between k_m and k_{cb} is about 2 orders of magnitude
- permeability drop occurs initially with formation of a few discrete compaction bands and further reduction is more gradual

Extrapolation of permeability evolution to other sandstones?

$$k_{eff} = \frac{k_m}{\left(\frac{nl}{L}\right)\left(\frac{k_m}{k_{cb}} - 1\right) + 1} = \frac{k_m}{\left(\frac{\varepsilon_p - \varepsilon_0}{\beta'}\right)\left(\frac{k_m}{k_{cb}} - 1\right) + 1}$$

$$\varepsilon_P = \varepsilon_0 + \beta \cdot n$$

$\beta = \Delta l / L$ ... nominal plastic strain associated with single band collapse

$\beta' = \Delta l / l$ ... localized plastic strain associated with single band collapse - serves here as material parameter

According to the model, permeability evolution with strain is dependent on $\gamma = (k_m/k_{cb} - 1)/\beta'$.

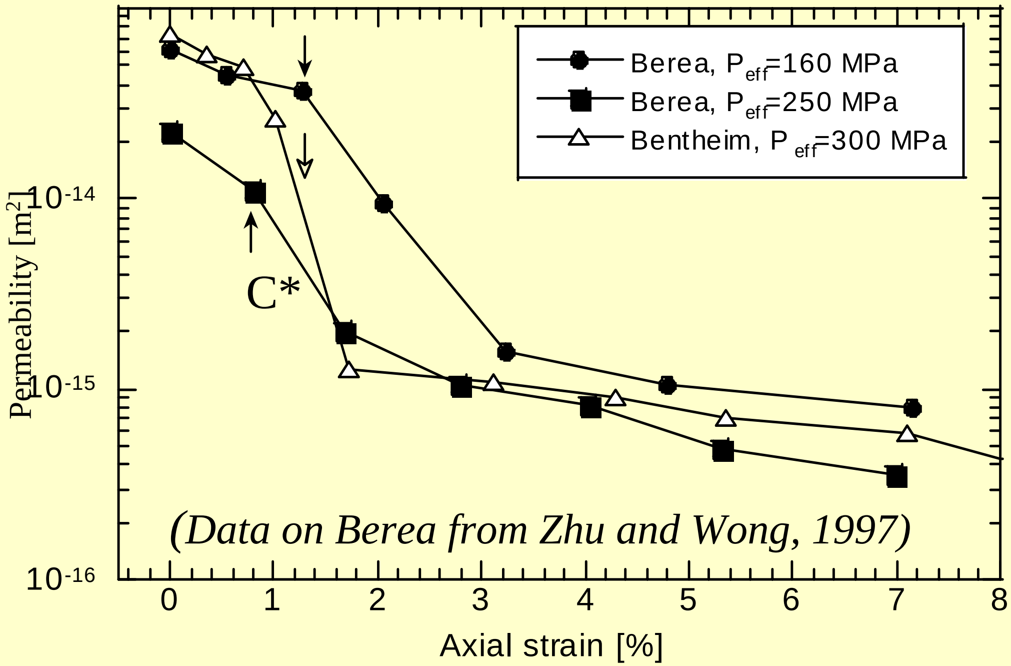

Comparison of Berea and Bentheim sandstones

Data indicate:

- smaller γ for Berea
- larger γ for Bentheim

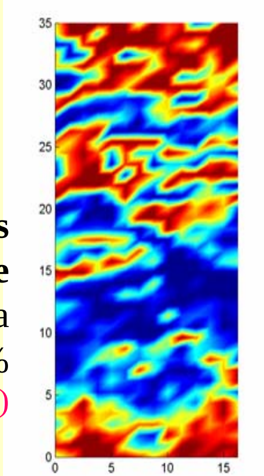

Diffuse compaction bands in Berea sandstone

P_{eff} = 200 MPa

ε_{axial} = 3.5%

(*Baud et al., 2004*)

Permeability evolution in Castlegate ($\phi = 28\%$)

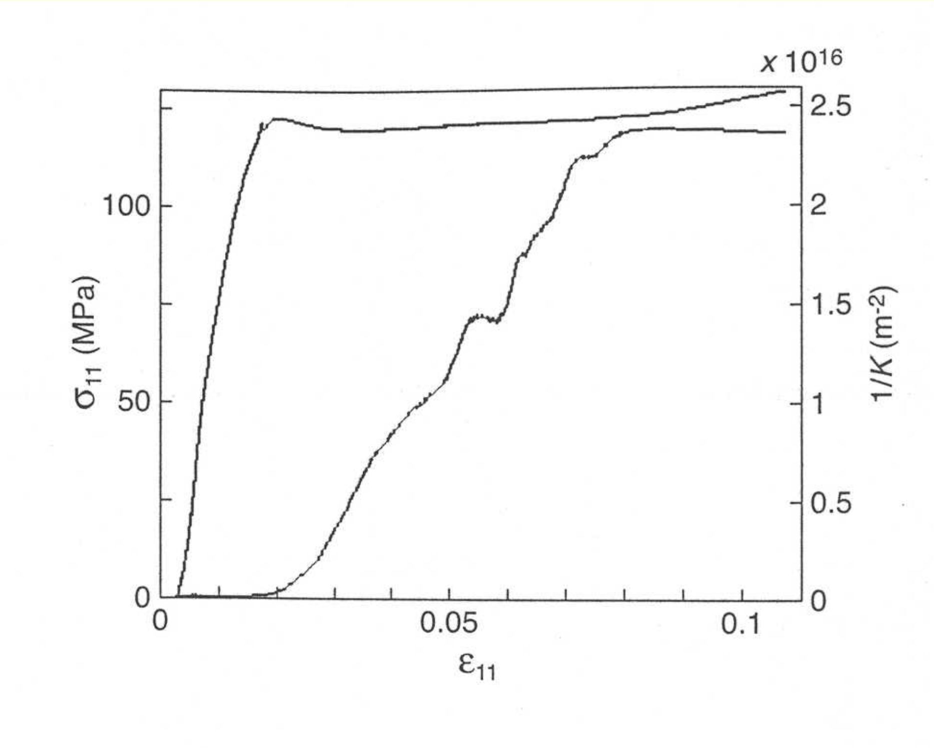

1/*k* is a linear function axial strain.

Holcomb and Olsson (2003)

Elastic waves velocities and compaction localization

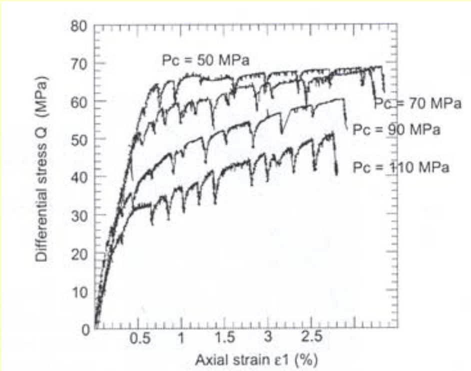

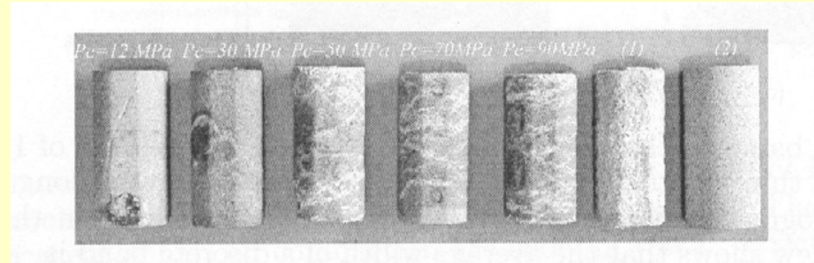

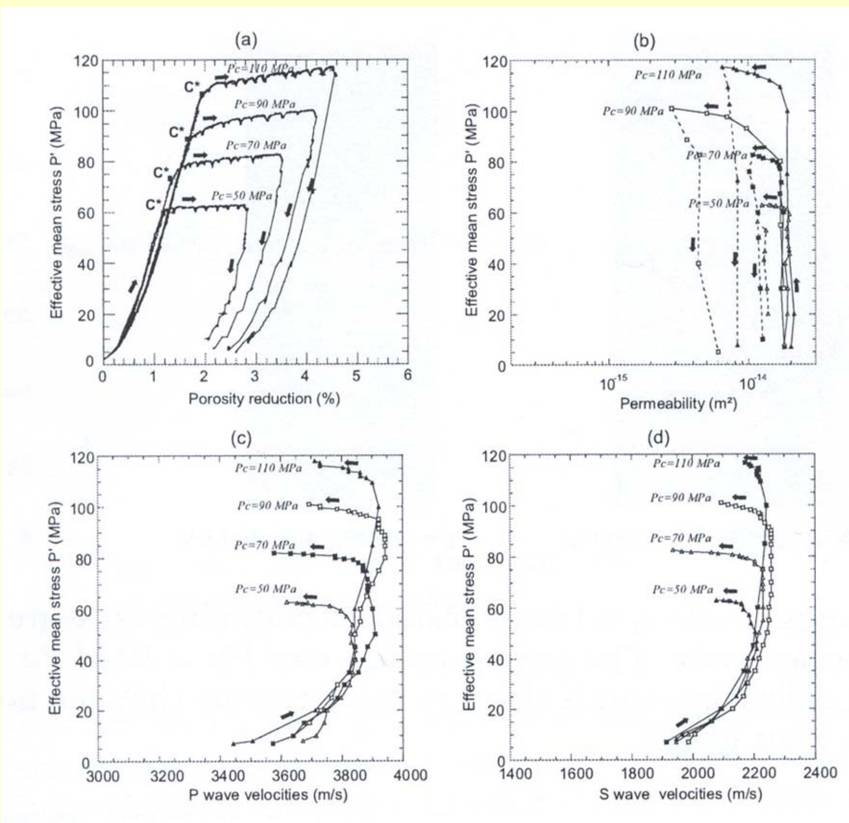

$$\frac{k_m}{k_{cb}} \sim \frac{\phi}{\overline{\zeta}} \in [6-600]$$

Inelastic compaction:
large increase in crack density
V_p and V_s decrease

Fortin et al. (2005)

V. Models

BIFURCATION ANALYSIS OF STRAIN LOCALIZATION

- **The inception of a localized zone of deformation is viewed as a *bifurcation* from homogenous deformation due to a *constitutive instability*** (*Rudnicki and Rice*, 1975). If g_k **is a** function of distance across the band, localized deformation in the form of a planar band with normal **n**, is possible if a non-trivial solution exists to the ***eigenvalue*** problem:

$$\{n_i L_{ijkl} n_l\}\, g_k = 0$$

- **Bifurcation Condition:** A ***nontrivial*** solution for the g_k is possible only when the following ***determinant*** vanishes

$$\det\{n_i L_{ijkl} n_l\} = 0$$

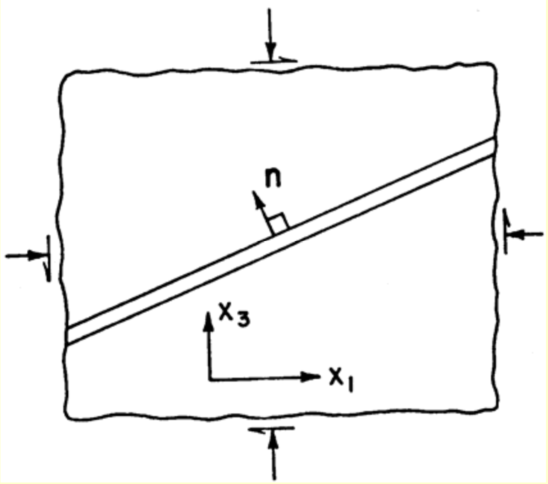

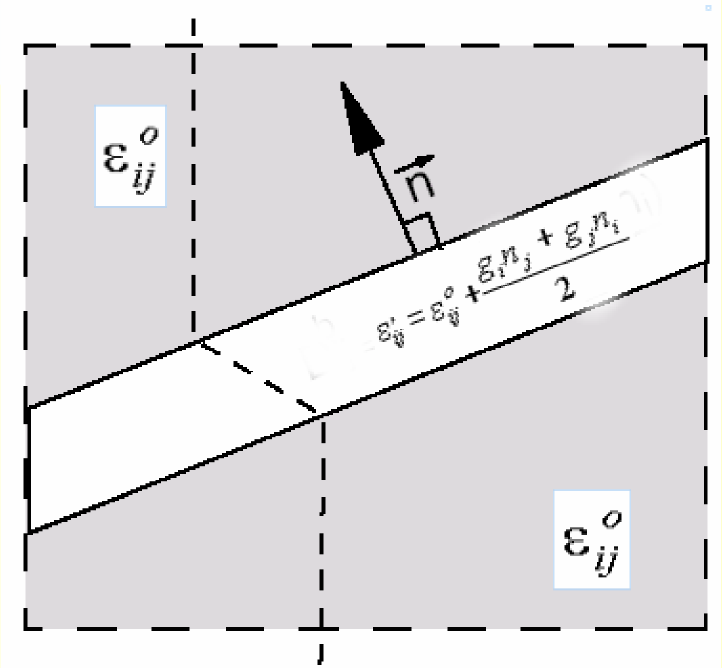

Bifurcation analysis of failure modes (for axisymmetric compression)

Rudnicki and Rice's constitutive parameters

β **dilatancy factor** (β <0 => compaction)

μ **friction coefficient** (μ <0 => negative pressure dependence)

$$\beta = -\sqrt{3}\,\frac{\Delta\phi^{p} / \Delta\varepsilon^{p}}{\left(3 - \Delta\phi^{p} / \Delta\varepsilon^{p}\right)}$$

$$\mu = -\frac{B^{2}\left(P - C\right)}{\sqrt{3}A^{2}Q}$$

Conditions for localization

☞ ***shear band*** *(Rudnicki and Rice, 1975; Perrin and Leblond, 1993)*

$$-\sqrt{3} \le \beta + \mu \le \sqrt{3}\,(2-\upsilon) / (1+\upsilon)$$

☞ ***compaction band*** *(Olsson, 2000; Issen and Rudnicki, 2000)*

$$\beta + \mu = -\sqrt{3}$$

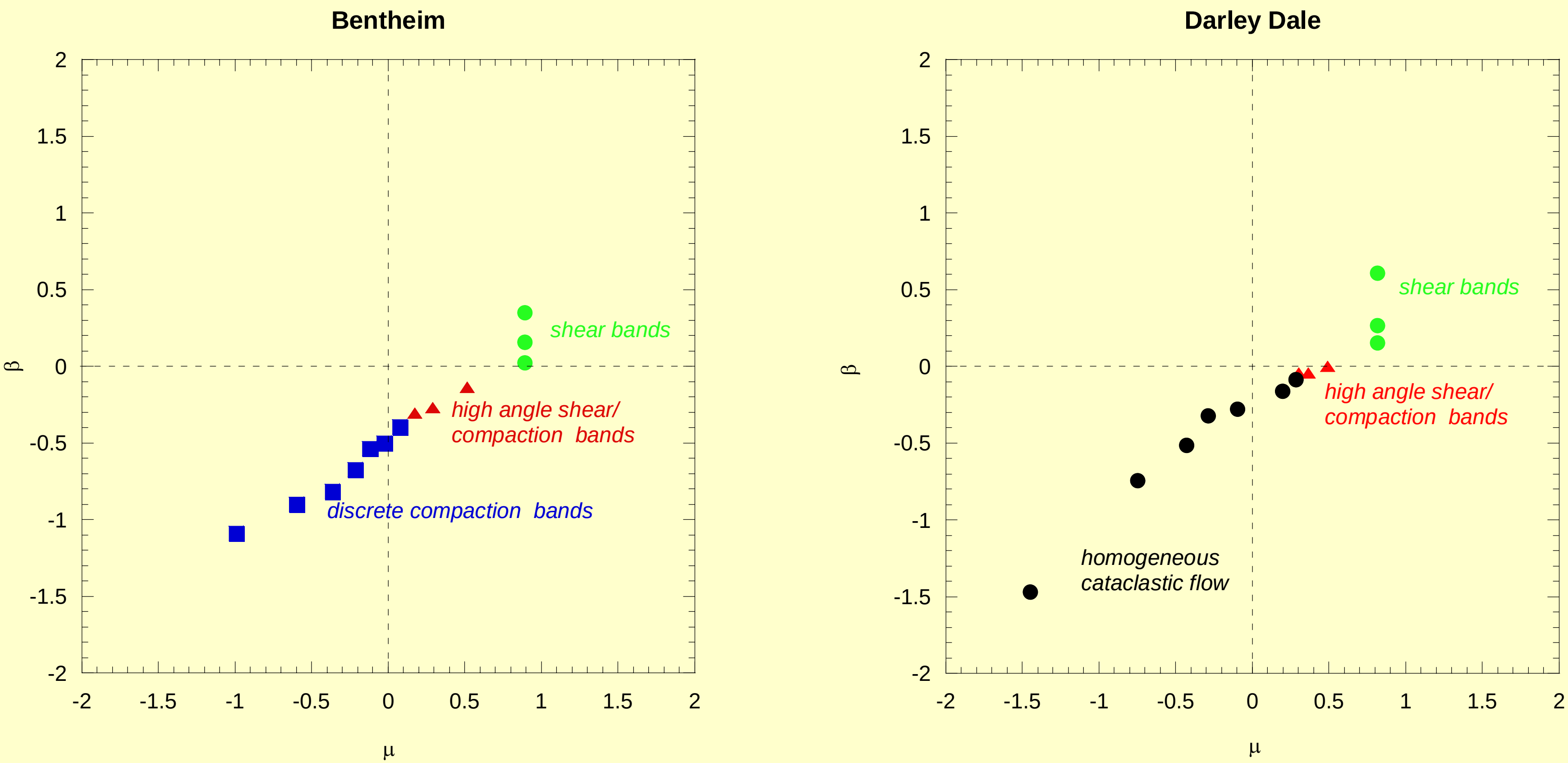

As a porous sandstone undergoes the brittle-ductile transition the failure mode evolves from shear band to compaction band to distributed cataclastic flow as the constitutive parameters β and μ decrease with increasing effective pressure.

Failure mode map from *Issen et Rudnicki* (2000)

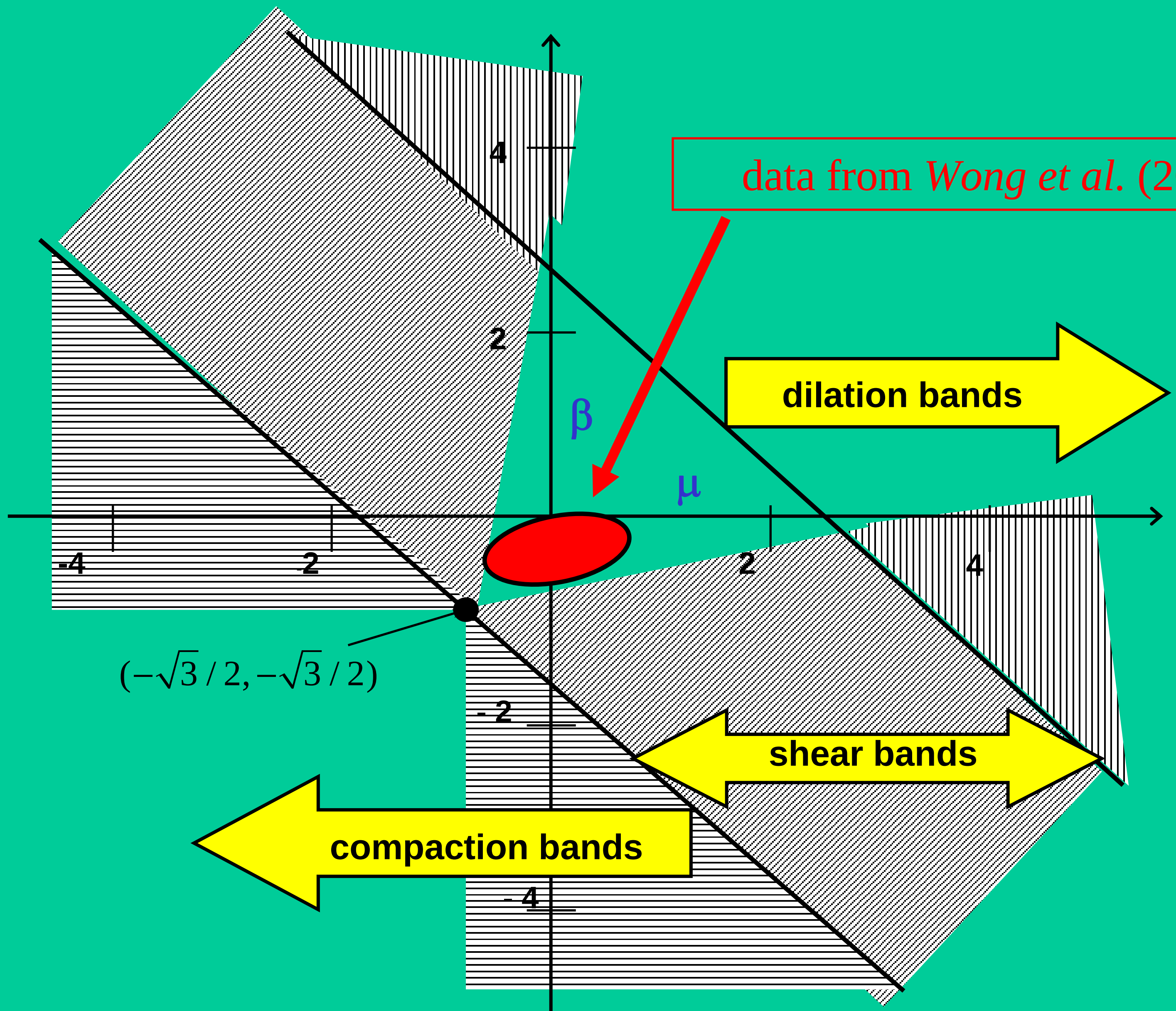

Wong, Baud et Klein (2001)

Poor agreement between theoretical predictions and laboratory data:

- theory only applies to onset of localization:
  - → AE location (*Fortin et al., 2005*)
- theoretical predictions for transverse isotropic material (*Rudnicki*, 2004)
  - → experiments using *exotic* stress paths (*Baud et al., in preparation*)
- heterogeneity of the stress field in the samples:
  - → study on notched samples (*Vajdova and Wong*, 2005; *Tembe et al., in press*)

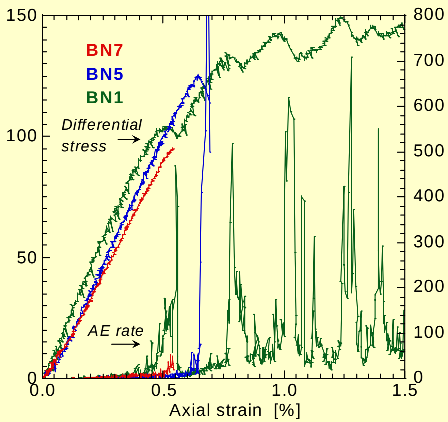

BN7

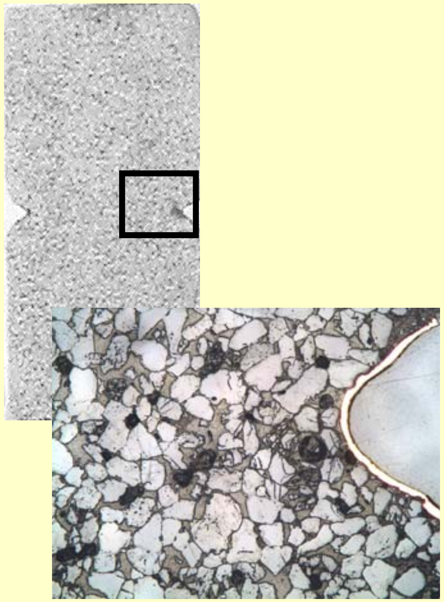

BN5

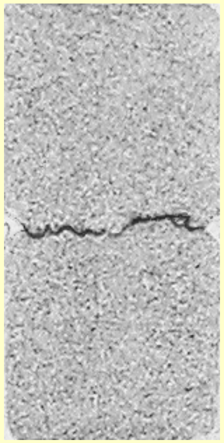

BN1

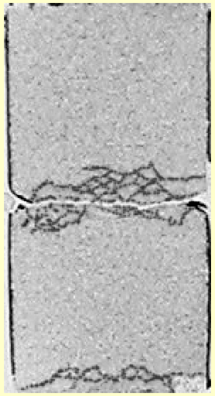

NETWORK MODELS:

hexagonal lattice of springs (*Katsman, Aharonov and Scher*, 2005)

no disorder

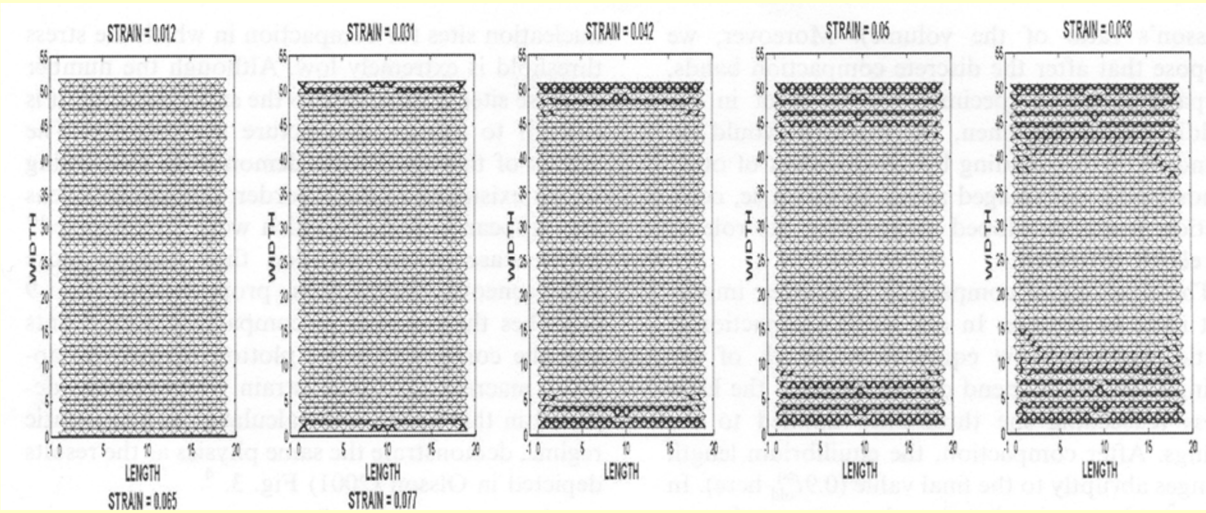

Bentheim

~ 100% quartz

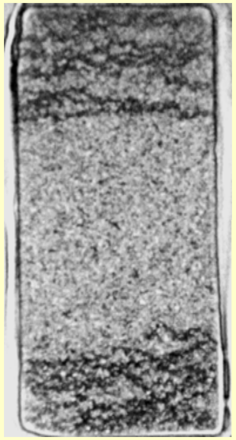

large disorder

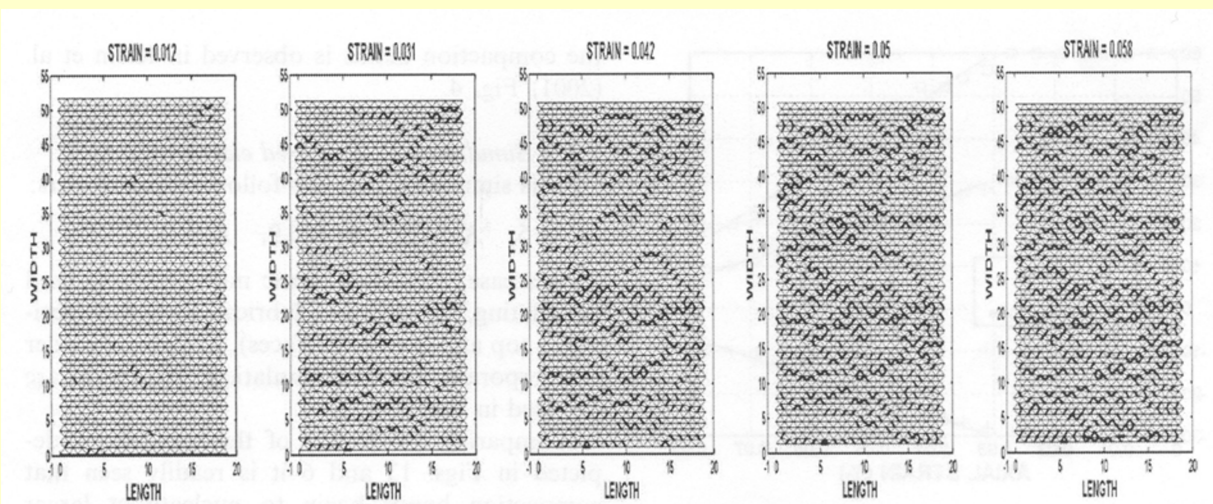

Dielmelstadt

68% quartz, 26% feld.

2-Dimensional Discrete Element Model:

The porous sandstone is modeled as a bonded assembly of circular disks subjected to 3 damage mechanisms: cohesion loss, relative movement among grains and intragranular cracking.

Geometric regularity tends to promote the development of discrete compaction bands in the DEM simulations

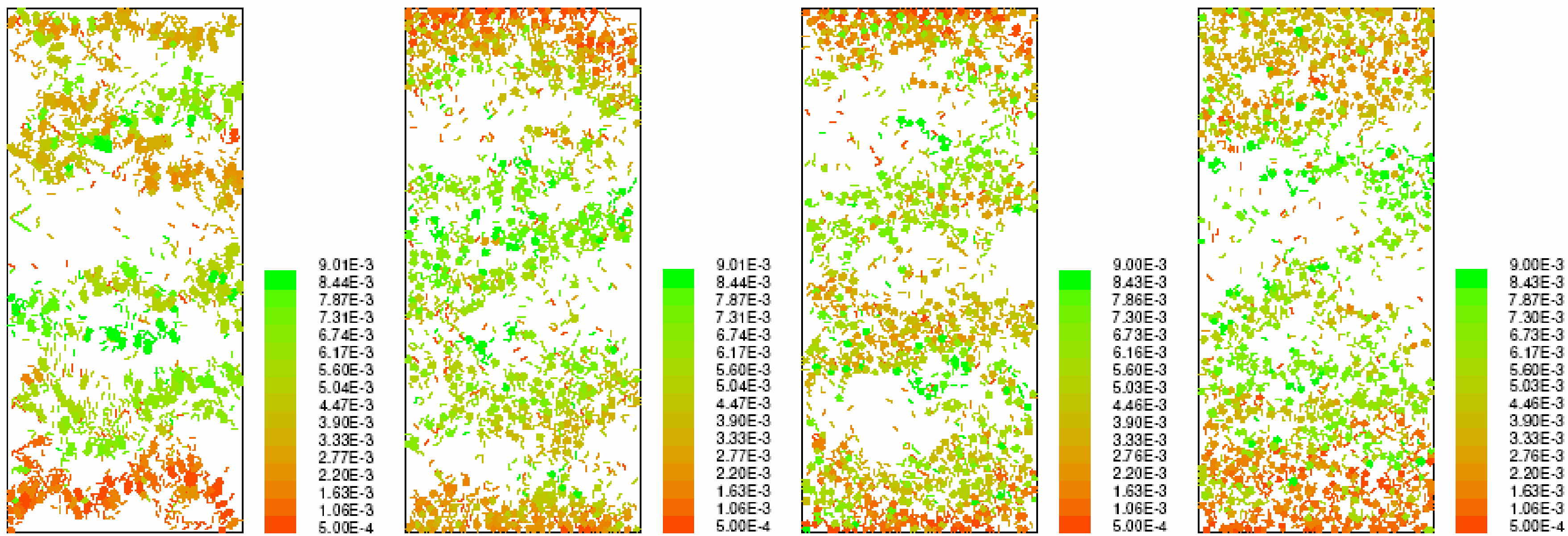

(a) R5r1, $\sigma_x = 70MPa$ (b) R45r12, $\sigma_x = 70MPa$ (c) R4r15, $\sigma_x = 70MPa$ (d) R33r2, $\sigma_x = 70MPa$

Wang, Chen and Wong (2005)

Conclusions

• Compaction localization was observable in most sandstones in the brittle-ductile transition.

• Several failure modes were observed:

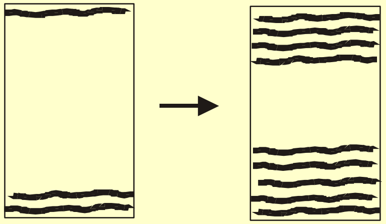

discrete compaction bands

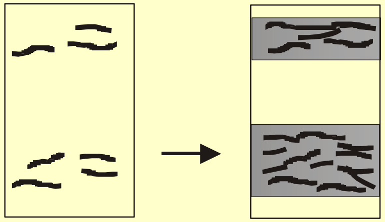

diffuse compaction bands

• Each failure mode has a typical AE signature.

• Permeability and its anisotropy are sensitively dependent on strain localization.

Future work

- mechanisms leading to nucleation and growth of compaction bands:
  - -AE location in Bentheim sandstone
  - -analysis of grain contacts
  - -tests on synthetic sandstones
- influence of heterogeneity and anisotropy
  - -network model with a disorder parameter *D*
  - -influence of sedimentary bedding on compaction localization
- impact of strain localization at reservoir scale
- compaction localization in carbonates ?

•Teng-fong Wong, Veronika Vajdova, Sheryl Tembe and Laurent Louis (*Stony Brook*)

•Emmanuelle Klein (*INERIS*)

•Jérôme Fortin (ENS Paris)

•Christian David (Cergy Pontoise)

•Pierre Bésuelle (INPG)

•Xiangyang Wu (*IGG/CAS, Beijing*)

•Kurt Sternlof (*Stanford*)

•Kathleen Issen (*Clarkson*) and John Rudnicki (*Northwestern*)

Failure mode map with two active yield surfaces (*Issen*, 2002)

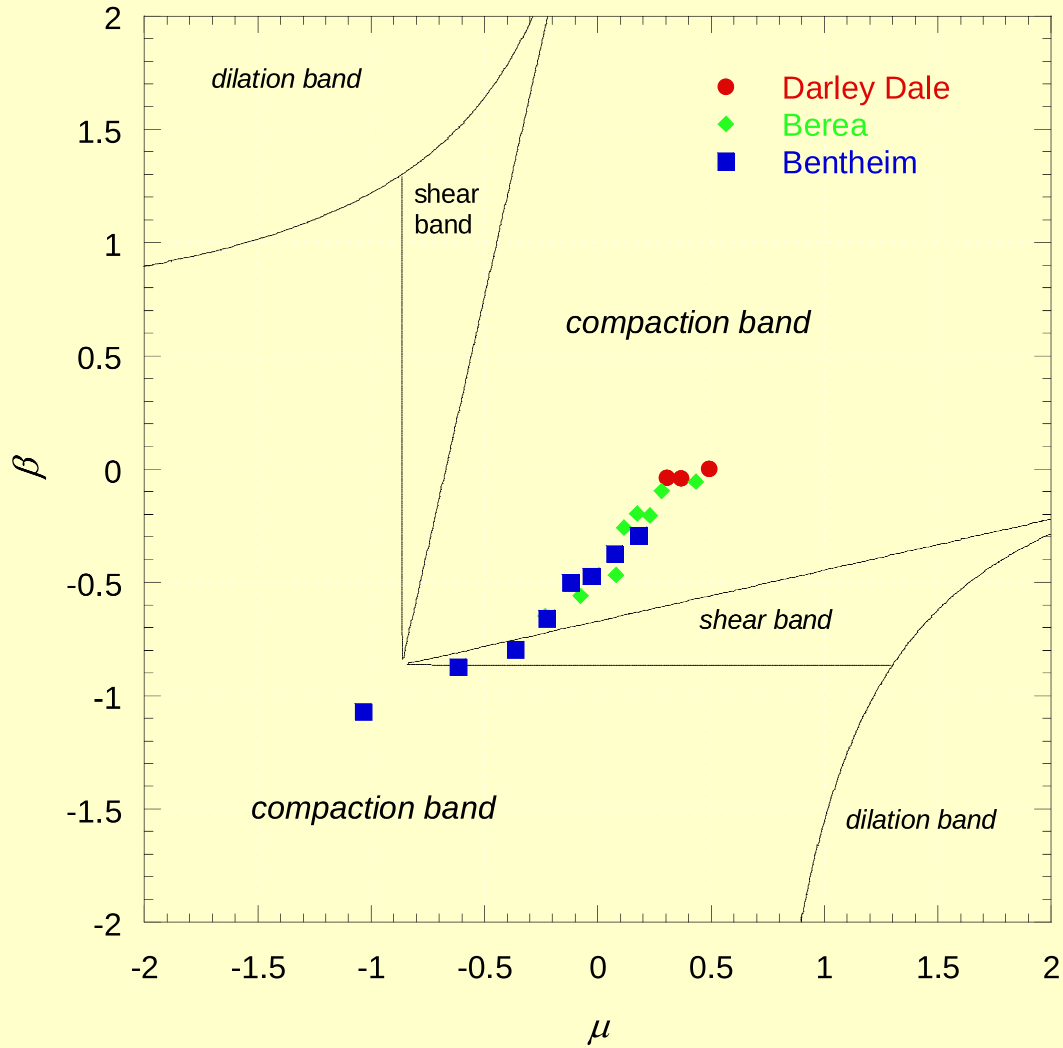

Baud, Vajdova and Wong (submitted)